

# Text4Seg++: Advancing Image Segmentation via Generative Language Modeling

Mengcheng Lan, Chaofeng Chen, *Member, IEEE*, Jiaxing Xu, Zongrui Li, Yiping Ke, *Member, IEEE*, Xudong Jiang, *Fellow, IEEE*, Yingchen Yu, Yunqing Zhao<sup>✉</sup>, Song Bai, *Member, IEEE*

**Abstract**—Multimodal Large Language Models (MLLMs) have shown exceptional capabilities in vision-language tasks. However, effectively integrating image segmentation into these models remains a significant challenge. In this work, we propose a novel *text-as-mask* paradigm that casts image segmentation as a text generation problem, eliminating the need for additional decoders and significantly simplifying the segmentation process. Our key innovation is *semantic descriptors*, a new textual representation of segmentation masks where each image patch is mapped to its corresponding text label. We first introduce *image-wise semantic descriptors*, a patch-aligned textual representation of segmentation masks that integrates naturally into the language modeling pipeline. To enhance efficiency, we introduce the Row-wise Run-Length Encoding (R-RLE), which compresses redundant text sequences, reducing the length of semantic descriptors by 74% and accelerating inference by 3 $\times$ , without compromising performance. Building upon this, our initial framework Text4Seg achieves strong segmentation performance across a wide range of vision tasks. To further improve granularity and compactness, we propose *box-wise semantic descriptors*, which localizes regions of interest using bounding boxes and represents region masks via structured mask tokens called semantic bricks. This leads to our refined model, Text4Seg++, which formulates segmentation as a next-brick prediction task, combining precision, scalability, and generative efficiency. Comprehensive experiments on natural and remote sensing datasets show that Text4Seg++ consistently outperforms state-of-the-art models across diverse benchmarks without any task-specific fine-tuning, while remaining compatible with existing MLLM backbones. Our work highlights the effectiveness, scalability, and generalizability of text-driven image segmentation within the MLLM framework.

**Index Terms**—Image segmentation, Multimodal large language models, Reasoning segmentation, Referring expression comprehension.

## I. INTRODUCTION

MULTIMODAL Large Language Models (MLLMs) [1] have significantly extended the capabilities of powerful Large Language Models (LLMs) into the visual domain. Recent advancements demonstrate their remarkable ability to perform natural language-based interaction and reasoning over visual inputs [2]–[6]. As a result, MLLMs are increasingly applied to a wide spectrum of vision-centric tasks, including image generation [7], [8], object detection [9]–[12] and semantic segmentation [13]–[15]. Despite these advances, seamlessly integrating MLLMs with these tasks, particularly

in dense prediction tasks like semantic segmentation, remains challenging due to the intrinsic differences between natural language and visual modalities.

A prevalent solution adopted by recent studies [11], [12], [15]–[20] involves appending additional visual decoders (e.g., SAM [21]) on top of MLLMs, as illustrated in Figure 1 (a). In such framework, an MLLM primarily functions as a multi-modal encoder that interprets user queries containing implicit or explicit references to regions of interest in an image. It then generates a special `<seg>` token that serves as a semantic cue and is processed jointly with visual features by a mask decoder to yield the final segmentation mask. While this paradigm has proven effective, it presents several drawbacks: 1) it complicates the end-to-end training pipeline with additional loss functions; 2) it requires careful modifications to MLLM architectures, leading to unexpected challenges when scaling up the training; and 3) it remains fundamentally discriminative, underutilizing the inherent generative capabilities of LLMs.

Another line of work [9], [22], [23] represents segmentation masks as polygon coordinate sequences that can be decoded in an autoregressive manner, aligning more closely with the language modeling paradigm. Notable examples include VisionLLM [9] and VistaLLM [22], illustrated in Figure 1 (b). Despite their conceptual elegance, these models often exhibit degraded performance, as LLMs struggle to associate coordinate sequences with accurate spatial shapes. This challenge has prompted the reintroduction of task-specific segmentation modules in improved variants like VisionLLMv2 [24]. These limitations underscore the pressing need for more effective strategies to unlock the full potential of MLLMs for segmentation tasks. Such method should adhere to the next-token prediction paradigm of MLLMs for easier optimization, minimize architectural modifications for scalability, and fully leverage text generation capabilities of LLMs.

In this paper, we introduce a novel *text-as-mask* paradigm that casts image segmentation as a text generation problem, which significantly simplifies the segmentation process, as illustrated in Figure 1 (c). At the core of this paradigm is a novel sequence representation of segmentation masks. Instead of using index masks or numerical coordinates, we map each flattened patch of the image to its corresponding text description (e.g., a semantic label, a short phrase, or a long sentence), forming a purely textual representation of images, named as **image-wise semantic descriptors** (I-SD). This representation offers several advantages: 1) a unified sequence representation seamlessly integrated into the auto-regressive training pipeline of MLLMs, making joint optimization with text tasks easier; 2)

✉ Corresponding Author: yunqing.z.0817@gmail.com.

Mengcheng Lan, Jiaxing Xu, Yiping Ke are with College of Computing and Data Science, Nanyang Technological University. Zongrui Li, Xudong Jiang are with School of Electrical and Electronic Engineering, Nanyang Technological University. Chaofeng Chen is with School of Artificial Intelligence, Wuhan University. Yingchen Yu, Yunqing Zhao, Song Bai are with ByteDance.

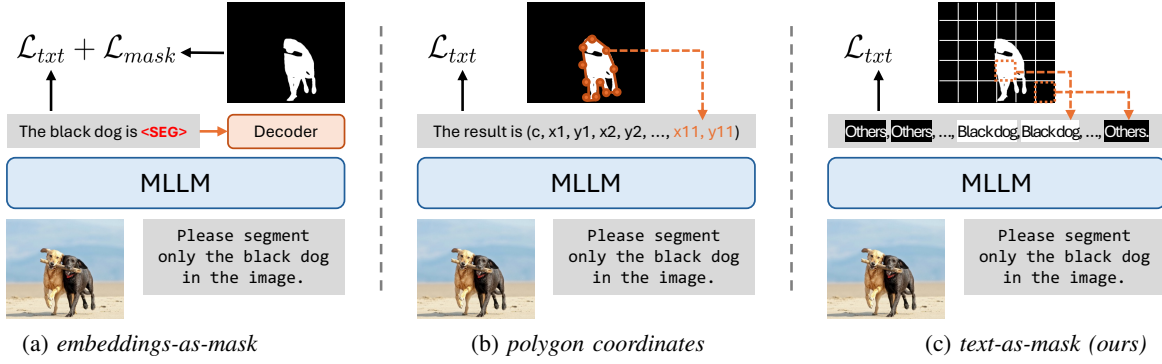


Fig. 1: Different paradigms of MLLMs based image segmentation: (a) *embeddings-as-mask* paradigm that relies on additional segmentation decoder and loss (e.g., LISA [15]); (b) *polygon coordinates* for image segmentation (e.g., VisionLLM [9] and VistaLLM [22]); (c) our *text-as-mask* paradigm that relies on semantically consistent text sequences.

no architectural changes are required, allowing full utilization of existing MLLMs training infrastructure, making it ideal for scaling up; 3) support for large label vocabularies, equivalent to semantic words; and 4) flexible switching between different kinds of image segmentation tasks.

Building upon our text-as-mask paradigm and image-wise semantic descriptors, we present our conference paper **Text4Seg** [25], a decoder-free segmentation framework that fully leverages the generative capabilities of MLLMs. Inspired by ViT [26], we demonstrate that *representing an image with  $16 \times 16$  semantic words, i.e., 256 length of semantic descriptors, is sufficient to achieve satisfactory results*. To improve efficiency, we introduce the Row-wise Run-Length Encoding (R-RLE), which losslessly compresses the repeated descriptors within each image row while preserving the spatial structure. Without compromising performance, R-RLE achieves a 74% reduction in semantic descriptors length and speeds up inference by  $3\times$  on average. To further enhance performance, we optionally apply an off-the-shelf mask refiner, e.g., SAM, as a post-processing step to obtain pixel-level segmentation masks.

While the image-wise semantic descriptors offers a global, patch-aligned representation well-suited for dense semantic segmentation, it still exhibits certain limitations: 1) repetitive textual descriptions, especially long sentences, inflate the sequence length and limit resolution scalability; 2) background tokens (e.g., "others") dominate the semantic descriptors, especially when segmenting small foreground objects in large scenes; and 3) it relies on explicit text labels for each image patch, making it less effective for reasoning-driven segmentation tasks without predefined semantics.

To address this, we propose a more focused and compact formulation: **box-wise semantic descriptors** (B-SD). This approach first localizes regions of interest using *tagged bounding boxes*, then it generates segmentation masks within each region using the semantic descriptors. By explicitly coupling *where* to look and *what* to segment, B-SD encapsulates both spatial and semantic information within a unified, autoregressive text format. B-SD eliminates the receptive textual descriptions by a single label tag, and minimizes the overhead of dense background tokens by the bounding box constraint. To further enhance expressiveness and efficiency, we extend the MLLM vocabulary with structured mask tokens, which we refer to as *semantic bricks*, (e.g.,  $\{fg1, fg2, \dots, fg63\}$ ,  $\{bg1,$

$bg2, \dots, bg63\}$ ), enabling segmentation to be interpreted as symbolic plotting on a  $64 \times 64$  canvas. Ultimately, this leads to our *next-brick prediction* framework: **Text4Seg++**, which generates box-wise semantic descriptors sequences brick-by-brick. Surprisingly, Text4Seg++ with  $64 \times 64$  B-SD not only achieves significantly finer-grained segmentation compared to  $16 \times 16$  I-SD in Text4Seg, but also reduces the overall sequence length. Additionally, Text4Seg++ preserves the elegance of generative language modeling with improved precision and scalability, opening new possibilities for dense prediction via pure text generation.

With the proposed semantic descriptors, training MLLMs for segmentation requires minimal additional effort. We begin by constructing instruction-following data from existing segmentation datasets, transforming the vanilla semantic masks into the semantic descriptors format, and then fine-tuning the model using query-response conversations. In our initial work [25], Text4Seg was fine-tuned and evaluated individually on each downstream segmentation task, demonstrating strong performance without any architectural changes.

In this work, we take a significant step further with Text4Seg++ by embracing a unified and generalizable framework, tailored for *conversational* image segmentation. We curate a large-scale, diverse training corpus that integrates a wide range of visual tasks, including referring expression segmentation, generalized referring expression segmentation, single- and multi-object reasoning segmentation, as well as visual grounding and understanding, across both natural and remote sensing imagery domains. This setup enables us to train a single, versatile MLLM segmentation model capable of performing robustly across tasks and domains *without the need for task-specific fine-tuning*. Our experiments demonstrate that Text4Seg++ can seamlessly integrate segmentation capabilities into existing MLLM architectures, such as Qwen2-VL [27], Deepseek-VL2 [28], and InternVL3 [29], *without any architectural modifications*. Without bells and whistles, Text4Seg++ consistently achieves superior performance to previous state-of-the-art methods, highlighting its efficiency, flexibility, and robustness. In summary, our key contributions are as follows:

#### In Text4Seg:

- We propose a novel *text-as-mask* paradigm formulating image segmentation as a text generation problem, which fully leverages the text generation capabilities of MLLMs.

- We introduce image-wise semantic descriptors, a patch-aligned textual representation of segmentation masks, and an efficient Row-wise Run-Length Encoding (R-RLE) to reduce sequence length and speed up inference. Built on this, Text4Seg achieves strong performance across diverse image segmentation tasks when conducting task-specific fine-tuning on different benchmarks.

#### In Text4Seg++:

- We further propose box-wise semantic descriptors, a focused region-level representation that unifies visual grounding and segmentation by jointly leveraging bounding boxes and semantic descriptors. This innovation is further bolstered by the introduction of semantic bricks, which significantly improve the compactness and decoding efficiency, enabling the generation of finer-grained, scalable segmentation masks with exceptional precision.
- We develop Text4Seg++, a unified and generalizable framework built upon our next-brick prediction. Text4Seg++ integrates diverse image segmentation and understanding tasks, allowing the training of a single, versatile model without any task-specific fine-tuning.
- Our method achieves state-of-the-art performance and robustness across a wide range of vision-centric tasks. Additionally, it demonstrates strong compatibility with various Multimodal Large Language Model (MLLM) backbones, highlighting its versatility and extensibility.

## II. RELATED WORK

### A. Multimodal Large Language Models

MLLMs are typically developed by enhancing large language models (LLMs) with visual perception modules, which can generate coherent textual conversations grounded in multimodal inputs. For instance, Flamingo [30] introduces the Perceiver Resampler, which connects a pre-trained vision encoder with LLMs for effective few-shot learning [31], [32]. BLIP-2 [33] and InstructBLIP [34] bridge the modality gap using a lightweight Querying Transformer (Q-Former), demonstrating enhanced performance on zero-shot vision-to-language tasks. The LLaVA series [2], [4] employs a linear layer or MLP as a modality connector, trained on multimodal language-image instruction-following data generated with GPT-4, showcasing notable capabilities in multimodal chat interactions. In contrast, Qwen-VL [5] and mPLUG-Owl2 [35] explore feature compression to a fixed length through cross-attention mechanisms with learnable queries. Recent advancements in multimodal modeling [27]–[29], [36]–[44] have focused on enhancing visual encoding through high-resolution inputs. For example, LLaVA-NEXT [36] and LLaVA-OneVision [38] utilize the AnyRes scheme to accommodate high-resolution image inputs. In contrast, Qwen2-VL [27] and Qwen2.5-VL [44] support native dynamic resolution through the introduction of a 2D-RoPE mechanism. Despite their strong visual capabilities in tasks such as general visual question answering, document understanding, OCR, and visually grounded agent applications, these MLLMs remain limited in their ability to perform dense prediction tasks, such as image segmentation. In this work, we present Text4Seg and Text4Seg++ to endow

existing MLLMs with image segmentation capabilities based on instruction tuning, *without necessitating any changes to their architecture.*

### B. MLLMs for Visual Segmentation

**Discriminative Models.** Recent advancements have enabled MLLMs to support image segmentation by incorporating task-specific modules *e.g.*, additional image encoder or mask decoder [21]. In these frameworks, MLLM primarily interprets user queries, which may contain implicit or explicit references to target objects in the image, and generate a special `<seg>` token that serves as a text-based cue. This cue, along with the visual features extracted by the image encoder, is then passed to the mask decoder, which produces the corresponding binary segmentation mask. A line of work, including LISA [15] and its successors [12], [16], [18]–[20], [45]–[47] adopt this *embedding-as-mask* paradigm and demonstrates strong performance on tasks such as reasoning segmentation and referring expression segmentation. This multimodal segmentation paradigm has also been extended to the remote sensing domain [48], [49]. In contrast, UFO [50] and Pixel-SAIL [51] propose to directly extract image embeddings from MLLMs and generate segmentation masks by computing the similarity between the image embeddings and text (*i.e.*, `<seg>`) embedding. However, this discriminative segmentation paradigm often complicates the end-to-end training pipeline due to the need for additional loss functions and architectural components.

**Generative Models.** Another major line of research investigates the strong generative capabilities of MLLMs for segmentation tasks. For example, HiMTok [52] and ALTo [53] use MLLMs to generate discrete mask tokens, which are then decoded via a mask detokenizer to produce fine-grained segmentation masks, achieving decent performance on various segmentation tasks. Other approaches [9], [22], [23] directly predict the polygon coordinates delineating object boundaries. However, these generative approaches often suffer from limited performance, as MLLMs may struggle to associate geometric representations (*e.g.*, polygon coordinates) with precise object shapes, leading to inaccurate or coarse masks.

### C. MLLMs for Visual Grounding

Visual grounding aims to localize specific objects in an image based on a natural language instructions, serving as a fundamental task that bridges vision and language modalities. Traditional approaches [54]–[56] typically frame it as a detection problem, employing task-specific architectures that combine object detection with language encoders to align textual phrases with corresponding image regions. Recent advances in MLLMs have enabled more flexible and general-purpose solutions to visual grounding. For instance, Kosmos-2 [57] and Shikra [58] discretize spatial locations by quantizing bounding boxes into either location tokens or numeric position representations. More recently, generalist MLLMs [10], [28], [29], [44], [59] have demonstrated the ability to directly predict bounding boxes as outputs in response to textual queries. In this work, we distinguish our approach from prior studies by binding bounding boxes with semantic masks, which provide



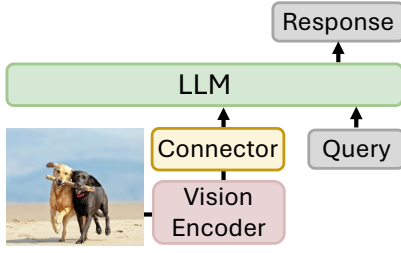


Fig. 2: An illustration of a popular MLLM architecture.

denser and more informative supervision signals. This enables the model to learn visual-linguistic alignments with improved granularity, ultimately enhancing both grounding precision and segmentation quality.

### III. METHODOLOGY

#### A. Preliminary

Multimodal Large Language Models (MLLMs) [1] refer to the LLM-based models with the ability to process, reason, and generate response from multimodal input information. Typically, as shown in Figure 2, an MLLM can be abstracted into three main components:

- *Vision Encoder*: A pre-trained vision encoder (e.g., CLIP [60] or SigLIP [61]) that transforms input images into a sequence of visual tokens.
- *Language Model*: A pre-trained large language model (LLM), such as Qwen3 [62] or LLaMA [63], responsible for understanding and generating natural language outputs through next-token prediction.
- *Modality Connector*: A bridging module that aligns visual and textual modalities. This is often implemented using lightweight architectures like a two-layer MLP [4] or cross-attention mechanisms [5], enabling effective fusion of visual features into the LLM’s context window.

#### B. Text4Seg with Image-wise Semantic Descriptors

1) *Definition of image-wise semantic descriptors*: Inspired by the patch-based representation of Vision Transformers (ViT) [26], our semantic descriptors encode segmentation masks into a sequence of semantic tokens spatially aligned with visual patches. As illustrated in Figure 3, the process begins by splitting the image into a grid of fixed-size patches (e.g.,  $16 \times 16$ ) and flattening them, resulting in 256 non-overlapping regions. Each patch is then represented by its corresponding semantic descriptor. A descriptor can be as simple as a semantic label (e.g., “sky”, “sand”), a phrase (e.g., “brown dog”, “black dog”), or even a more complex textual description (e.g., “a brown dog on the left side”) for intricate scenes. This design choice transforms an image into a sequence of image-wise semantic descriptors (I-SD) of length 256, which meets the requirements for integrating image segmentation into MLLMs and offers several key advantages:

- It naturally aligns with the next-token prediction paradigm of existing LLMs, reframing image segmentation as a standard generative language modeling task, facilitating easier optimization.

- It requires no modifications to existing MLLMs architecture, making it easily scalable and compatible with existing training infrastructures.
- It adopts a *text-as-mask* paradigm, fully using the text generation capabilities of LLMs for image segmentation.

One of the key limitations of full-length image-wise semantic descriptors lies in its substantial token length, which stems from the spatial redundancy inherent in pixel-aligned representations. For instance, on the RefCOCO [64] dataset, the average token length of 256-I-SD is 583, requiring approximately 19s on an NVIDIA V100 GPU for a single round of referring expression segmentation.

2) *Image-wise RLE*: To address this inefficiency, we explore the simple Run-Length Encoding (RLE) [65], a classic compression technique, to reduce redundant tokens in the sequence. A naïve solution is to apply RLE directly across the entire semantic descriptors sequence, referred to as Image-wise RLE (I-RLE), as shown in Figure 3. However, we empirically found that it results in a notable performance degradation, dropping nearly 4 cIoU on the RefCOCO *val* split. This indicates that compressing the semantic descriptors globally may disrupt essential two-dimensional spatial patterns that MLLMs rely on for accurate segmentation.

3) *Row-wise RLE*: To mitigate this issue, we propose a novel Row-wise Run-Length Encoding (R-RLE) technique. As shown in Figure 3, R-RLE compresses adjacent repeated descriptors within each row of the semantic descriptor grid, with each row separated by “\n”. This approach reduces the token length from 583 to 154 on average while preserving more spatial information. Importantly, R-RLE demonstrates no performance degradation compared to the full-length semantic descriptors, and significantly enhances the inference speed.

4) *Visual Instruction Tuning*: Building upon the proposed I-SD, we construct visual instruction data by repurposing existing segmentation annotations into an instruction-following format. Figure 4 illustrates a few examples from referring expression segmentation. Given an `<image, mask>` pair, we first resize the segmentation mask to a fixed  $16 \times 16$  resolution and flatten it into a 1D sequence. The numerical labels in the sequence are then replaced with their corresponding text labels to create full-length semantic descriptors. To reduce redundancy and improve efficiency, we further apply R-RLE to compress the sequence, with descriptors separated by “|” and rows separated by “\n”. Finally, we wrap the image input, textual labels (e.g., class names or referring expressions), and the compressed descriptors into an instruction-following query-response format as shown below:

#### Instruction-response template

**Query:** `<image>` Can you segment the `<text labels>` in the image?

**Response:** The result is: \n `<seg>`image-wise semantic descriptors`</seg>`.

Here, `<image>` is a placeholder for the visual input tokens, while `<seg>` and `</seg>` are special markers indicating the start and end of the semantic descriptors sequence.

## Image patches



## Semantic descriptors

sky, sky, sky, sky, sky, sky, sky, sky, sky, sky, sky, sky, sky, sky, sky, brown dog, black dog, sky, sky, sky, sky, brown dog, black dog, black dog, sky, sand, sand, brown dog, black dog, black dog, sand, sand, sand, brown dog, black dog, sand, sand


## Image-wise RLE

sky\*14, brown dog\*1, black dog\*1, sky\*4, brown dog\*1, black dog\*2, sky\*1, sand\*2, brown dog\*1, black dog\*2, sand\*3, brown dog\*1, black dog\*1, sand\*2

## Row-wise RLE

sky\*6 \n sky\*6 \n sky\*2, brown dog\*1, black dog\*1, sky\*2 \n sky\*2, brown dog\*1, black dog\*2, sky\*1 \n sand\*2, brown dog\*1, black dog\*2, sand\*1 \n sand\*2, brown dog\*1, black dog\*1, sand\*2 \n

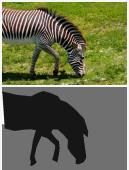
Fig. 3: An illustration of image patches, image-wise semantic descriptors and two token compression techniques.



**Query:** Can you segment the *dog laying down* in the image?

**Response:** The segmentation mask for 'dog laying down' is shown below:  
 $\text{<seg>others *16\n others *16\n others *16\n others *16\n others *16\n others *16\n dog laying down *1| others *15\n dog laying down *4| others *12\n dog laying down *5| others *11\n dog laying down *7| others *9\n others *16\n others *16\n others *16\n </seg>}$

---



**Query:** Please segment the image and highlight *'zebra, grass'*.

**Response:** Here is the segmentation map focusing on the zebra, grass:  
 $\text{<seg>grass *16\n zebra *2| grass *2| zebra *3| grass *9\n zebra *8| grass *8\n zebra *9| grass *7\n zebra *10| grass *6\n zebra *10| grass *6\n zebra *11| grass *5\n zebra *11| grass *5\n grass *4| zebra *2| grass *1| zebra *4| grass *5\n grass *4| zebra *3| grass *1| zebra *2| grass *6\n grass *4| zebra *1| grass *1| zebra *1| grass *1| zebra *3| grass *5\n grass *8| zebra *3| grass *5\n grass *9| zebra *2| grass *5\n grass *6| zebra *1| grass *2| zebra *2| grass *5\n grass *9| zebra *1| grass *6\n grass *16\n </seg>}$

Fig. 4: Visual instruction tuning data based on image-wise semantic descriptors.

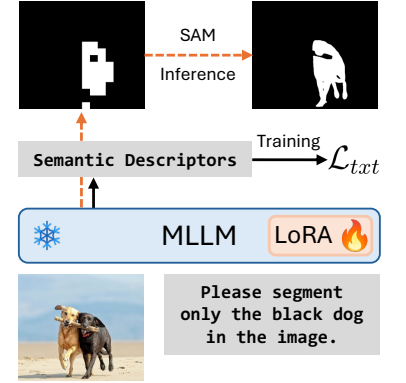


Fig. 5: Text4Seg architecture.

5) *Text4Seg Architecture*: With such text-only response design, Text4Seg can be seamlessly integrated with existing MLLMs without any architectural modifications, as shown in Figure 5. We use Low-Rank Adaptation (LoRA) [66] to fine-tune the MLLMs on our visual instruction data, using its original auto-regressive training objective  $\mathcal{L}_{txt}$  [2]. In contrast to existing models [15], [17], [20], which typically rely on Continued Pre-Training (CPT) with large, mixed datasets to fuse the architectures before fine-tuning on specific downstream tasks, we directly apply Supervised Fine-Tuning (SFT) on the downstream tasks. During inference, to obtain a better pixel-level semantic mask, we optionally apply SAM as the mask refiner with our generated coarse mask as its prompt.

## C. Text4Seg++ with Box-wise Semantic Descriptors

1) *Motivation*: While the image-wise semantic descriptors provide a global, patch-aligned textual representation well-suited for dense semantic segmentation, and Text4Seg demonstrates strong performance across individual segmentation tasks, it still faces several limitations:

- *Redundant textual descriptions*: Repetitive semantic descriptors, especially full-sentence annotations, result in unnecessarily long token sequences. This increases computational overhead and hinders scalability to higher-resolution inputs, ultimately limiting fine-grained segmentation performance.
- *Background token dominance*: In scenes with large backgrounds and small foreground objects, the semantic de-

scriptors are often dominated by background tokens (e.g., "others"), reducing the semantic density and expressiveness of the representation.

- *Dependency on explicit labels*: Image-wise semantic descriptors require explicit semantic labels for each patch, which becomes limited in reasoning-driven tasks (e.g., reasoning segmentation) where semantics are context-dependent or inferred. This restricts generalization to tasks beyond fixed label spaces.

To address these limitations, we introduce a more compact representation: box-wise semantic descriptors (B-SD).

2) *Definition of box-wise semantic descriptors*: We reformulate image segmentation as a two-step process: visual grounding followed by visual segmentation. Based on this formulation, we introduce a novel representation, box-wise semantic descriptors, to describe each segmented instance in a compact and structured textual format, as illustrated in Figure 6(a). Specifically, each instance is represented using the following syntax:

## Box-wise semantic descriptor

```
<ref>text labels</ref><box>[[x1 y1 x2 y2]]
</box><seg>semantic descriptors</seg>
```

where  $\text{<ref>}$ ,  $\text{</ref>}$ ,  $\text{<box>}$ ,  $\text{</box>}$ ,  $\text{<seg>}$  and  $\text{</seg>}$  are special tokens. This representation consists of three core components:

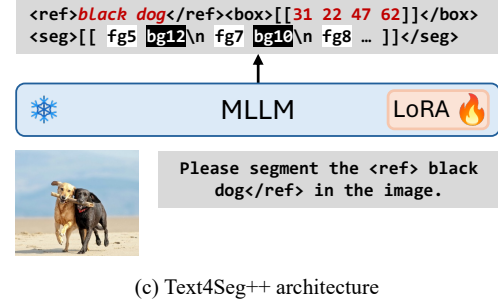
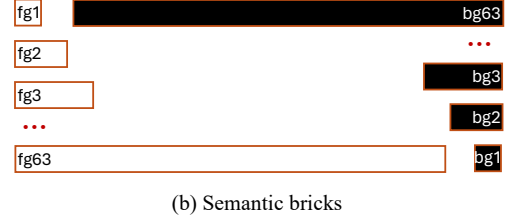
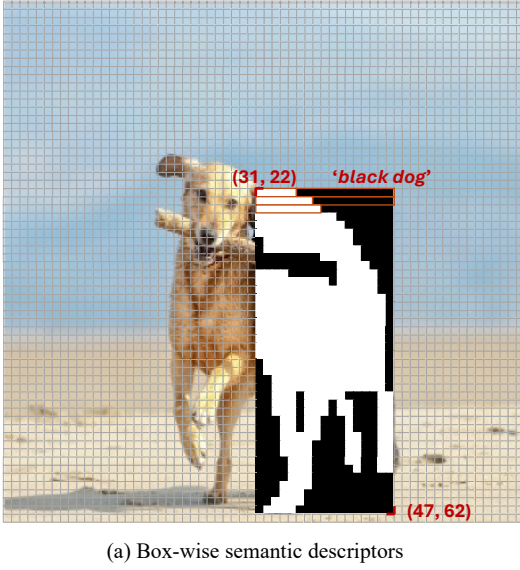


Fig. 6: An illustration of (a) box-wise semantic descriptors for images, (b) semantic bricks and (c) Text4Seg++ framework.

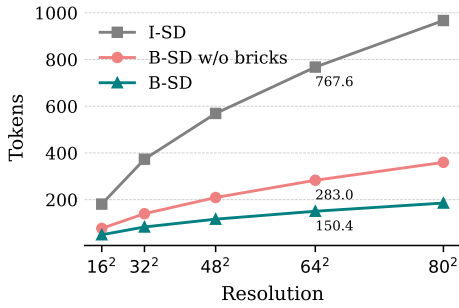


Fig. 7: Token counts with varying resolution of semantic descriptors for three configurations: I-SD, B-SD, and B-SD without semantic bricks.

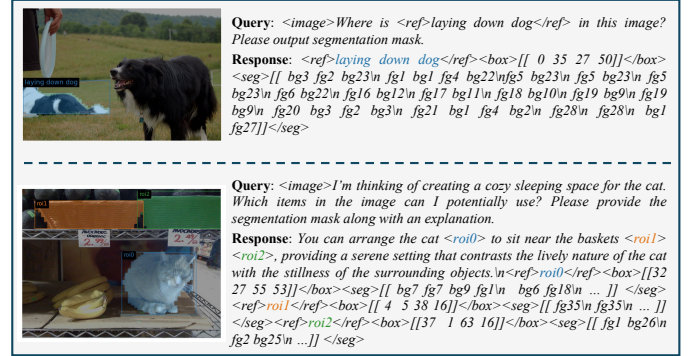


Fig. 8: Visual instruction tuning data based on box-wise semantic descriptors.

- `<ref>...</ref>`: A natural language referring the expression or category label that provides semantic grounding for the object (e.g., “black dog”, “the person on the left”). To support scenarios without explicit labels, such as reasoning segmentation where object identity is context-dependent, we introduce abstract region identifiers (e.g., `roi0`, `roi1`, ...). This strategy mitigates the issue of repetitive semantic descriptors and alleviates the reliance on explicit labels.
- `<box>...</box>`: The bounding box coordinates of the object, formatted as `[[x1 y1 x2 y2]]`, where `(x1, y1)` and `(x2, y2)` represent the top-left and bottom-right corners, respectively. Each coordinate is quantized into one of 64 discrete bins, aligning with the resolution of the semantic descriptors. By localizing the region of interest, this structure effectively reduces the dominance of background tokens and ensures that the model focuses on semantically meaningful regions.
- `<seg>...</seg>`: A concise semantic descriptors of the object mask.

Together, these components provide a compact yet informative textual representation that supports efficient and generalizable dense segmentation.

3) *Next Brick Prediction*: While our R-RLE significantly reduces the length of semantic descriptors, there is still room for further compression. Empirically, we observe that each semantic block can span multiple tokens. For instance, the string `others*16` is tokenized into four separate tokens, “others”, “\*”, “1” and “6”, when using the Qwen [62] tokenizer. This token-level granularity introduces unnecessary overhead in both sequence length and decoding time.

To further enhance the compactness and decoding efficiency of the semantic descriptors, we introduce a set of special tokens, referred to as *semantic bricks*, as illustrated in Figure 6(b). Specifically, we construct a vocabulary of 126 bricks: 63 white foreground bricks (denoted as `fg1`, `fg2`, ..., `fg63`) and 63 black background bricks (denoted as `bg1`, `bg2`, ..., `bg63`). Each brick corresponds to a binary segment of varying lengths, encoding the object mask in a compact and interpretable form. To reconstruct the full mask from these bricks, we adopt a sequential generation strategy, referred to as *next brick prediction*, where the model predicts one brick at a time to construct the binary mask. The bricks are arranged from left to right and top to bottom, mimicking the raster-scan order of a 2D mask. This design not only reduces token count



and improves inference speed but also aligns well with the autoregressive generation paradigm of large language models.

We quantitatively compare the token lengths of image-wise and box-wise semantic descriptors representations using the Qwen tokenizer on the RefCOCO dataset, as shown in Figure 7. The results reveal that the box-wise formulation is significantly more compact. For instance, at a resolution of  $64 \times 64$ , the average token length of B-SD without semantic bricks is 283.0, substantially shorter than the 767.6 tokens required by the image-wise counterpart. Furthermore, incorporating semantic bricks into the B-SD reduces the token length even further to 150.4. These findings demonstrate the token efficiency and scalability of our box-wise semantic descriptors.

In Figure 8, we present two qualitative examples of visual instruction response. These examples illustrate that our proposed B-SD is effective not only for image segmentation tasks with explicit labels (e.g., referring expression segmentation) but also for tasks without explicit supervision, such as reasoning-driven segmentation. This highlights the generality and versatility of our framework in both low-level and high-level segmentation scenarios.

4) *Text4Seg++ Architecture*: As illustrated in Figure 6(c), Text4Seg++ maintains the architectural simplicity of Text4Seg by leveraging a pure text-based output format, enabling seamless integration with existing MLLMs without any structural modifications. Specifically, Text4Seg++ generates high-resolution B-SD as autoregressive text responses, enabling more fine-grained and spatially precise segmentation. To support this higher-resolution output, it is essential that the input image also maintains sufficient resolution. Consequently, we adopt MLLM architectures capable of processing high-resolution visual inputs, such as Qwen2-VL-7B [27] and InternVL3-8B [29], ensuring high fidelity in both visual encoding and textual decoding. We use LoRA to perform post-training on the MLLMs using the pure generative language modeling loss.

## IV. EXPERIMENTS

### A. Experiment Setup

1) *Implementation Details*: Our methods are designed to be seamlessly integrated into existing Multimodal Large Language Model (MLLM) architectures. For Text4Seg, we adopt InternVL2-8B [6] and LLaVA-1.5-13B [4] as base models. For Text4Seg++, we employ Qwen2-VL-7B [27], which natively supports dynamic input resolutions and demonstrates higher optimization efficiency. All MLLM architectures are kept unchanged during the experiments. Additionally, we optionally incorporate SAMRefiner [67] with a ViT-H backbone as an off-the-shelf mask refinement module.

Our methods are implemented using SWIFT framework [68]. Text4Seg++ is trained on 8 NVIDIA H100 GPUs with a global batch size of 128. We use the AdamW optimizer [69], starting with an initial learning rate of  $2e-4$ , which follows a linear decay schedule after a warm-up phase with a ratio of 0.03. The weight decay is set to 0, and gradient norms are clipped at 1.0. To minimize GPU memory usage, we fine-tune all models using LoRA with a rank of 128, along with ZeRO-1 stage memory optimization [70].

TABLE I  
STATISTICS OF THE TRAINING DATA.

Dataset	Task Description	#Image	#Sample
COCO	panoptic segmentation	118k	236k
refCOCO	referring expression segmentation	74k	439k
	referring expression comprehension		
grefCOCO	generalized referring expression segmentation	17k	209k
Pix2Cap	referring expression segmentation	18k	152k
ReasonSeg	single-object reasoning segmentation	209	1045
MUSE	multi-object reasoning segmentation	102k	230k
	remote sensing referring		
RRSIS_D	image segmentation & grounding	12k	61k
Earthreason	geospatial reasoning segmentation	2.4k	71k
LLaVA-665k	visual understanding	665k	665k

2) *Evaluation Protocol*: We adopt a comprehensive set of metrics to evaluate the effectiveness of our proposed methods:

- **cIoU** (Cumulative IoU) [71]: Computes the cumulative intersection over cumulative union across all samples. This metric favors larger objects by aggregating pixel-level overlap globally.
- **gIoU** (Generalized IoU) [72]: Calculates the mean per-image IoU across all samples. For no-target cases, true positive predictions are assigned an IoU of 1, while false negatives are assigned 0. This metric provides a balanced assessment of performance on both small and large objects.
- **mIoU** (Mean IoU): Similar to gIoU, it computes the average per-image IoU across the dataset.
- **ACC@0.5**: Accuracy of the IoU between the predicted and ground truth bounding boxes thresholds at 0.5, reflecting the referring expression comprehension.
- **Accuracy**: Measures the correctness of the model's answers in the visual question answering task, assessing multimodal understanding and reasoning capabilities.

This diverse set of metrics allows for a thorough evaluation of visual segmentation grounding and understanding.

### B. Datasets

Following prior work in multimodal image segmentation [15], [17], [20], we train Text4Seg++ on a diverse collection of datasets. Specifically, we construct our training data using the method introduced in Section III-C, leveraging the following datasets:

- **COCO Panoptic Segmentation** [79] is a comprehensive segmentation dataset that includes 80 *thing* categories (e.g., dogs, cats) and 91 *stuff* categories (e.g., grass, sky). We use the training split containing approximately 118,000 images.
- **refCOCO series** includes several single-object referring expression segmentation datasets: RefCLEF, RefCOCO, RefCOCO+ [64], and RefCOCOg [73]. We use the train splits for all datasets.
- **grefCOCO** [72] is a generalized referring expression segmentation dataset designed for multi-object and no-target segmentation tasks. It consists of 278k expressions, including 80k multi-target and 32k no-target expressions.
- **Pix2Cap** [80] contains approximately 20,000 images and 167,254 captions. We treat the caption corresponding to each mask as a referring expression. We use the training split, which includes 18,212 images.

TABLE II

REFERRING EXPRESSION SEGMENTATION RESULTS (cIoU) ON REF-COCO (+/G) [64], [73] BENCHMARKS. MASK DEC.: MASK DECODER. U: THE UMD PARTITION. FT: MODELS ARE FINETUNED ON THE JOINT TRAINING SPLIT OF THE REFERRING EXPRESSION SEGMENTATION DATASETS. <sup>†</sup> MODEL BASED ON THE 32× 32 I-SD WITHOUT THE MASK REFINER. <sup>‡</sup> MODEL BASED ON THE 64× 64 B-SD WITHOUT THE MASK REFINER. THE BEST RESULTS ARE HIGHLIGHTED IN **RED**, WHILE THE SECOND-BEST RESULTS ARE MARKED WITH **SECOND**.

Method	LLM	Mask Dec.	val	refCOCO testA	refCOCO testB	val	refCOCO+ testA	refCOCO+ testB	refCOCOg val(U)	refCOCOg test(U)	Avg.
<i>Specialised Segmentation Models</i>											
ReLA [CVPR23] [72]	BERT	✓	73.8	76.5	70.2	66.0	71.0	57.7	65.0	66.0	68.3
PolyFormer-L [CVPR23] [74]	BERT	✗	76.0	78.3	73.3	69.3	74.6	61.9	69.2	70.2	71.6
UNINEXT-L [CVPR24] [56]	BERT	✓	80.3	82.6	77.8	70.0	74.9	62.6	73.4	73.7	74.4
LAVT [TPAMI24] [75]	BERT	✓	79.2	80.7	75.4	71.7	75.6	64.3	72.1	74.6	74.2
<i>Generalist Segmentation Models (7B)</i>											
NEXT-Chat (FT) [ICML24] [12]	Vicuna-7B	✓	74.7	78.9	69.5	65.1	71.9	56.7	67.0	67.0	68.9
LISA (FT) [CVPR24] [15]	Vicuna-7B	✓	74.9	79.1	72.3	65.1	70.8	58.1	67.9	70.6	69.9
GSVA (FT) [CVPR24] [16]	Vicuna-7B	✓	77.2	78.9	73.5	65.9	69.6	59.8	72.7	73.3	71.4
PixelLM [CVPR24] [19]	Vicuna-7B	✓	73.0	76.5	68.2	66.3	71.7	58.3	69.3	70.5	69.2
AnyRef (FT) [CVPR24] [18]	LLaMA2-7B	✓	76.9	79.9	74.2	70.3	73.5	61.8	70.0	70.7	72.2
Groundhog [CVPR24] [17]	LLaMA2-7B	✓	78.5	79.9	75.7	70.5	75.0	64.9	74.1	74.6	74.2
GLaMM (FT) [CVPR24] [20]	Vicuna-7B	✓	79.5	83.2	76.9	72.6	78.7	64.6	74.2	74.9	75.6
SAM4MLLM [ECCV24] [76]	Vicuna-7B	✓	79.8	82.7	74.7	<b>74.6</b>	80.0	67.2	75.5	76.4	76.4
OMG-LLaVA (FT) [NeurIPS24] [45]	InterLM2-7B	✓	78.0	80.3	74.1	<b>69.1</b>	73.1	63.0	72.9	72.9	72.9
VITRON (FT) [NeurIPS24] [59]	Vicuna-7B	✓	75.5	79.5	72.2	66.7	72.5	58.0	67.9	68.9	70.2
M <sup>2</sup> SA [ICLR25] [46]	Vicuna-7B	✓	74.0	76.8	69.7	63.1	67.2	56.1	67.0	68.3	67.8
SETOKIM [ICLR25] [11]	LLaMA2-7B	✓	-	-	-	68.0	72.4	61.2	71.3	71.3	-
SegLLM [ICLR25] [47]	Vicuna-7B	✓	80.2	81.5	75.4	70.3	73.0	62.5	72.6	73.6	73.6
SegAgent (FT) [CVPR25] [77]	Qwen-7B	✓	79.7	81.4	76.6	72.5	75.8	66.9	75.1	75.2	75.4
POPEN [CVPR25] [78]	Vicuna-7B	✓	79.3	82.0	74.1	73.1	77.0	65.1	75.4	75.6	75.2
VistaLLM [CVPR24] [22]	Vicuna-7B	✗	74.5	76.0	72.7	69.1	73.7	64.0	69.0	70.9	71.2
Text4Seg <sup>†</sup> (FT) [25]	InterLM2-7B	✗	74.7	77.4	71.6	68.5	73.6	62.9	70.7	71.6	71.4
Text4Seg (FT) [25]	InterLM2-7B	✓	79.2	81.7	75.6	72.8	77.9	66.5	74.0	75.3	75.4
Text4Seg++ <sup>‡</sup>	Qwen2-7B	✗	<b>81.5</b>	<b>83.6</b>	<b>79.6</b>	<b>76.9</b>	<b>81.2</b>	<b>71.4</b>	<b>79.6</b>	<b>80.4</b>	<b>79.3</b>
Text4Seg++	Qwen2-7B	✓	<b>81.6</b>	<b>84.1</b>	<b>78.9</b>	<b>76.9</b>	<b>81.7</b>	<b>70.9</b>	<b>78.2</b>	<b>78.9</b>	<b>78.9</b>
<i>Generalist Segmentation Models (≥13B)</i>											
LISA (FT) [CVPR24] [15]	Vicuna-13B	✓	76.0	78.8	72.9	65.0	70.2	58.1	69.5	70.5	70.1
GSVA (FT) [CVPR24] [16]	Vicuna-13B	✓	78.2	80.4	74.2	67.4	71.5	60.9	74.2	75.6	72.8
M <sup>2</sup> SA [ICLR25] [46]	LLaMA2-13B	✓	74.6	77.6	71.0	64.0	68.1	57.6	69.0	69.3	68.9
VistaLLM [CVPR24] [22]	Vicuna-13B	✗	77.2	78.7	73.9	71.8	74.4	65.6	69.8	71.9	72.3
Text4Seg (FT) [25]	Vicuna-13B	✓	80.2	82.7	77.3	73.7	78.6	67.6	74.0	75.1	76.2
Text4Seg++ <sup>‡</sup>	Qwen2.5-14B	✗	<b>81.6</b>	<b>83.7</b>	<b>79.3</b>	<b>77.3</b>	<b>81.3</b>	<b>72.5</b>	<b>80.7</b>	<b>80.8</b>	<b>79.7</b>
Text4Seg++	Qwen2.5-14B	✓	<b>82.5</b>	<b>84.9</b>	<b>79.5</b>	<b>77.9</b>	<b>82.5</b>	<b>72.6</b>	<b>79.4</b>	<b>79.7</b>	<b>79.9</b>

- **ReasonSeg** [15] is a single-target reasoning segmentation dataset comprising 1,218 image-instruction-mask samples. The dataset is divided into train, val, and test splits containing 239, 200, and 779 samples, respectively.
- **MUSE** [19] is a multi-target reasoning segmentation dataset with 246,000 question-answer pairs, averaging 3.7 targets per answer. It is split into 239k training, 2.8k validation, and 4.3k test samples.
- **RRSIS\_D** [81] is a large-scale dataset for Remote Sensing Referring Image Segmentation (RRSIS), containing 17,402 image-mask-expression triplets. All images are at a resolution of 800 × 800 pixels.
- **Earthreason** [48] is a geospatial pixel-level reasoning dataset designed to evaluate complex real-world remote sensing scenarios. It consists of 5,434 manually annotated image-mask pairs and over 30,000 implicit question-answer pairs, covering 28 scene categories.
- **LLaVA-665k** [4] is a visual instruction-following dataset that contains 665k multimodal samples designed to enhance vision-language reasoning capabilities.

We summarize the statistics of our training data in Table I. To advance toward a general-purpose image segmentation framework, we train Text4Seg++ on the unified benchmark for 50k steps and evaluate its performance across diverse downstream tasks, **without any task-specific fine-tuning**.

## C. Main Results

1) *Referring Expression Segmentation*: We conduct a comprehensive evaluation of our methods on the RefCOCO family of benchmarks and present comparative results in Table II. Among 7B-scale discriminative models equipped with mask decoders, GLaMM achieves an average performance of 75.6 cIoU across eight evaluation splits, closely followed by POPEN, which utilizes preference-based optimization and obtains 75.2 cIoU. SAM4MLLM also demonstrates strong results, achieving the second-best performance on 5 out of 7 individual splits, and ranks second overall in average performance. For 7B-scale generative models that operate without mask decoders, our Text4Seg achieves an average of 71.4 cIoU, marginally outperforming VistaLLM (71.2 cIoU), which generates polygon coordinates to represent segmentation masks. Remarkably, our proposed Text4Seg++, even without any mask refinement, achieves a significantly higher average of 79.3 cIoU, outperforming the second-best model (76.4 cIoU) by nearly 3 points. Text4Seg++ delivers the best performance on all eight evaluation splits, establishing a new state-of-the-art among both discriminative and generative models at this scale. When scaled to 13B MLLMs, both Text4Seg++ and Text4Seg continue to demonstrate strong generalization. Text4Seg++ achieves an average of 79.7 cIoU,



TABLE III  
GENERALIZED REFERRING EXPRESSION SEGMENTATION RESULTS ON THE GREFCOCO [72] BENCHMARK. <sup>†</sup> MODEL BASED ON THE 32× 32 I-SD WITHOUT THE MASK REFINER. <sup>‡</sup> MODEL BASED ON THE 64× 64 B-SD WITHOUT THE MASK REFINER.

Method	LLM	Mask Dec.	Validation Set gIoU	Validation Set cIoU	Test Set A gIoU	Test Set A cIoU	Test Set B gIoU	Test Set B cIoU	Avg.
<i>Specialised Segmentation Models</i>									
ReLA [CVPR23] [72]	BERT	✓	63.6	62.4	70.0	69.3	61.0	59.9	64.4
LAVT [TPAMI24] [75]	BERT	✓	58.4	57.6	65.9	65.3	55.8	55.0	59.7
<i>Generalist Segmentation Models (7B)</i>									
LISA (FT) [CVPR24] [15]	Vicuna-7B	✓	61.6	61.8	66.3	68.5	58.8	60.6	62.9
GSVA (FT) [CVPR24] [16]	Vicuna-7B	✓	66.5	63.3	71.1	69.9	62.2	60.5	65.6
SAM4MLLM [ECCV24] [76]	Vicuna-7B	✓	71.9	67.8	<u>74.2</u>	<u>72.2</u>	65.3	63.2	69.1
Text4Seg <sup>†</sup> (FT) [25]	InternLM2-7B	✗	71.8	65.6	71.2	70.0	64.2	62.5	67.6
Text4Seg (FT) [25]	InternLM2-7B	✓	<b>74.4</b>	69.1	<b>75.1</b>	<b>73.8</b>	<b>67.3</b>	<b>66.6</b>	<b>71.1</b>
Text4Seg++ <sup>‡</sup>	Qwen2-7B	✗	73.5	<u>69.3</u>	72.7	71.9	<u>65.8</u>	<u>65.6</u>	69.8
Text4Seg++	Qwen2-7B	✓	<u>73.9</u>	<b>69.4</b>	73.5	<u>72.2</u>	65.7	65.3	<u>70.0</u>
<i>Generalist Segmentation Models (≥13B)</i>									
LISA (FT) [CVPR24] [15]	Vicuna-13B	✓	63.5	63.0	68.2	69.7	61.8	62.2	64.7
GSVA (FT) [CVPR24] [16]	Vicuna-13B	✓	68.0	64.1	71.8	70.5	63.8	61.3	66.6
Text4Seg <sup>†</sup> (FT) [25]	Vicuna-13B	✗	70.3	66.9	69.8	71.4	63.8	64.4	67.8
Text4Seg (FT) [25]	Vicuna-13B	✓	<b>74.8</b>	<b>69.8</b>	<b>75.1</b>	<b>74.3</b>	<b>68.0</b>	<b>67.1</b>	<b>71.5</b>
Text4Seg++ <sup>‡</sup>	Qwen2.5-14B	✗	73.4	<u>69.1</u>	72.2	71.1	65.7	65.2	69.5
Text4Seg++	Qwen2-7B	✓	<u>74.1</u>	<b>69.8</b>	<u>73.5</u>	<u>72.1</u>	<u>65.9</u>	<u>65.5</u>	<u>70.2</u>

TABLE IV  
REASONING SEGMENTATION RESULTS ON THE REASONSEG [15] BENCHMARK.

Method	LLM	Val gIoU	Val cIoU	Test gIoU	Test cIoU	Avg.
LISA [CVPR24] [15]	Vicuna-7B	53.6	52.3	48.7	48.8	50.9
SegLLM [ICLR25] [47]	Vicuna-7B	57.2	<b>54.3</b>	52.4	48.4	53.1
Seg-Zero [Arxiv25] [82]	Qwen2.5-7B	<b>61.6</b>	<u>52.6</u>	<b>58.2</b>	<b>52.4</b>	<b>56.2</b>
Text4Seg++	Qwen2-7B	<u>59.1</u>	49.5	<u>57.1</u>	<u>52.1</u>	<u>54.5</u>

TABLE V  
MULTI-TARGET REASONING SEGMENTATION RESULTS ON THE MUSE [19] BENCHMARK.

Method	LLM	Val gIoU	Val cIoU	Test gIoU	Test cIoU	Avg.
LISA [CVPR24] [15]	Vicuna-7B	17.2	28.8	24.4	36.5	26.7
GSVA [CVPR24] [16]	Vicuna-7B	38.9	40.9	44.3	54.1	44.6
PixelLM [CVPR24] [19]	Vicuna-7B	41.9	48.9	44.0	57.8	48.2
POPEN [CVPR25] [78]	Vicuna-7B	<u>45.4</u>	<u>55.2</u>	<u>46.4</u>	<u>62.9</u>	<u>52.5</u>
Text4Seg++	Qwen2-7B	<b>70.4</b>	<b>57.7</b>	<b>63.2</b>	<b>63.8</b>	<b>63.8</b>

while Text4Seg follows closely with 76.2 cIoU, both significantly surpassing other competing models, including the generative VistaLLM (72.3 cIoU). These results highlight the effectiveness and scalability of our text-as-mask framework and demonstrate the superiority of Text4Seg++ in referring expression segmentation. By leveraging the box-wise semantic descriptors and next-brick prediction, Text4Seg++ delivers a compact yet expressive textual representation that supports scaling up both mask resolution and training data.

2) *Generalized Referring Expression Segmentation*: We further evaluate our methods on generalized referring expression segmentation benchmark, which includes both multi-object and no-object cases, as shown in Table III. Without any

TABLE VI  
OPEN VOCABULARY SEGMENTATION RESULTS (mIoU) ON VARIOUS IMAGE SEGMENTATION BENCHMARKS.

Method	ADE-150 mIoU	PC-59 mIoU	PAS-20 mIoU
<i>Specialised Segmentation Models</i>			
ClearCLIP [ECCV24] [83]	16.7	35.9	80.9
ProxyCLIP [ECCV24] [84]	24.2	39.6	83.3
MaskCLIP [ICML23] [85]	23.7	45.9	-
GroupViT [CVPR22] [86]	9.2	23.4	79.7
OVSeg [CVPR23] [87]	24.8	53.3	92.6
SAN [TPAMI23] [88]	27.5	53.8	94.0
<i>Generalist Segmentation Models (7B)</i>			
LaSagnA [Arxiv24] [89]	14.3	46.1	69.8
Text4Seg [ICLR25] [25]	<b>16.5</b>	<b>52.5</b>	<b>76.5</b>

task-specific design, both Text4Seg and Text4Seg++ maintain strong performance in this more challenging setting. At the 7B scale, Text4Seg++ without the mask refiner achieves an average score of 69.8, outperforming GSVA (65.6) by over 4 points and exceeding Text4Seg without mask refinement (67.6). However, when equipped with a mask refiner and fine-tuned exclusively on this benchmark, Text4Seg achieves a higher average of 71.1, surpassing Text4Seg++. At the 13B scale, Text4Seg further extends its lead, achieving an average of 71.5, outperforming GSVA by 4.9 points, while Text4Seg++ records a strong 69.5. These results underscore the robustness and versatility of our Text4Seg and Text4Seg++ in handling more complex segmentation scenarios involving multiple or absent referents.

3) *Reasoning Segmentation*: We further assess the conversational image segmentation capabilities of Text4Seg++ on two challenging benchmarks specifically designed to assess reasoning segmentation in vision-language models. For a fair comparison with all baselines that incorporate mask

TABLE VII  
REFERRING EXPRESSION SEGMENTATION RESULTS ON THE RRSIS-D [81] BENCHMARK.

Method	LLM	Validation Set			Test Set			Avg.
		Acc@0.5	gIoU	cIoU	Acc@0.5	gIoU	cIoU	
Specialised Models								
RMSIN [CVPR24] [81]	BERT	74.7	65.1	78.3	74.3	64.2	77.8	72.4
LAVT [TPAMI24] [75]	BERT	69.5	61.5	77.6	69.5	61.0	77.2	69.4
Generalist Models								
LISA [CVPR24] [15]	Vicuna-7B	27.1	27.8	-	24.5	26.8	-	-
PixelLM [CVPR24] [19]	Vicuna-7B	33.5	33.7	-	28.8	31.7	-	-
NEXT-Chat [ICML24] [12]	Vicuna-7B	29.0	27.0	-	26.4	25.0	-	-
GeoGround [Arxiv24] [90]	Vicuna-7B	68.7	61.1	-	67.5	60.5	-	-
SegEarth-R1 (FT) [Arxiv25] [48]	Phi-1.5-1.3B	78.6	67.6	78.9	77.0	66.4	78.0	74.4
Text4Seg++	Qwen2-7B	74.8	64.1	75.8	73.2	62.8	74.2	70.8

TABLE VIII  
GEOSPATIAL PIXEL REASONING RESULTS ON THE EARTHREASON [48] BENCHMARK.

Method	LLM	Val		Test		Avg.
		gIoU	cIoU	gIoU	cIoU	
Generalist Models						
LISA (FT) [15]	Vicuna-7B	61.0	57.4	60.9	59.1	59.6
PixelLM (FT) [19]	Vicuna-7B	57.9	57.8	60.0	59.2	58.7
SegEarth-R1 (FT) [48]	Phi-1.5-1.3B	68.6	64.1	70.8	68.3	68.0
Text4Seg++	Qwen2-7B	71.9	69.8	73.0	65.6	70.1

decoders, we equip Text4Seg++ with SAMRefiner as an off-the-shelf post-processing mask refiner. The first benchmark, ReasonSeg [15], focuses on complex reasoning grounded in world knowledge and requires models to handle implicit, compositional, or abstract query texts. As shown in Table IV, Text4Seg++ achieves an average score of 54.5, significantly outperforming LISA (50.9), and performing comparably to SegLLM (53.1). However, it slightly underperforms SegZero (56.2), which benefits from a dedicated reasoning-chain-guided segmentation mechanism tailored for this task.

The second benchmark, MUSE [19], presents a more complex multi-object reasoning segmentation challenge. As reported in Table V, Text4Seg++ significantly outperforms all existing baselines by a large margin, achieving an average score of 63.8. This is 11.3 points higher than the best-performing baseline, POPEN (52.5), and dramatically outperforms early models like LISA (26.7), GSVA (44.6), and PixelLM (48.2). Built purely on generative language modeling, Text4Seg++ achieves superior reasoning ability, segmentation precision, and multi-object understanding without requiring architectural customization.

4) *Open Vocabulary Segmentation:* We follow LaSagna [89] to evaluate the performance of Text4Seg on open-vocabulary segmentation tasks. We evaluate the model's performance on ADE20K (A-150) [91], PASCAL Context 59 (PC-59) [92], and PASCAL VOC 20 (PAS-20) [93] datasets, using mIoU as the evaluation metric.

As demonstrated in Table VI, it is expected that Text4Seg falls behind specialized segmentation models (e.g., ProxyCLIP [84], OVSeg [87], and SAN [94]), because LLMs typically require quite large datasets to be sufficiently trained. However, Text4Seg still demonstrates competitive performance on the

PC-59 benchmark, underscoring its efficiency. More importantly, it significantly outperforms the MLLM-based LaSagna, which uses an additional decoder, showcasing its strong potential for open-vocabulary segmentation.

5) *Extend to Remote Sensing Image Segmentation:* To further evaluate the generalization ability of Text4Seg++ beyond natural images, we conduct experiments on remote sensing image segmentation tasks. We consider two challenging benchmarks. On RRSIS-D [81] shown in Table VII, which focuses on referring expression segmentation in remote sensing scenes, Text4Seg++ achieves an average score of 70.8, closely approaching the best-performing specialized models, including RMSIN (72.4). It underperforms the best-performing specialized model, SegEarth-R1 (74.4), despite being trained with a unified formulation and no domain-specific finetuning. Compared to previous vision-language models such as GeoGround, Text4Seg++ demonstrates significantly better localization and semantic understanding in high-resolution aerial imagery.

EarthReason [48] benchmark is a recently introduced task designed to assess precise geospatial pixel reasoning ability. As shown in Table VIII, Text4Seg++ achieves a new state-of-the-art performance with an average score of 70.1. This surpasses the strong baseline SegEarth-R1 (68.0) and significantly outperforms PixelLM (58.7) and LISA (59.6). These results highlight the scalability, domain transferability, and robust reasoning capabilities of our text-as-mask framework in diverse settings, including complex geospatial environments. Notably, Text4Seg++ achieves this performance without any architectural modification or remote-sensing-specific module, reinforcing its potential as a unified segmentation solution across domains.

6) *Referring Expression Comprehension:* As Text4Seg++ leverages the box-wise semantic descriptors formulation, it naturally unifies visual grounding and segmentation within a single, compact representation. To assess its capacity for referring expression comprehension, we evaluate the model's ability to localize referred objects using bounding boxes, measured by the standard Acc@0.5 metric. Experiments are conducted on the widely used RefCOCO benchmarks. As shown in Table IX, Text4Seg++ achieves superior performance across all evaluation splits compared to both specialized and generalist baselines. At the 7B scale, Text4Seg++ sets a new state-of-the-art with an average Acc@0.5 of 91.1, outperforming the strongest prior model, InternVL3 (89.7).

TABLE IX  
REFERRING EXPRESSION COMPREHENSION RESULTS (ACC@0.5) ON REF-COCO (+/G) [64], [73] BENCHMARKS.

Method	LLM	val	refCOCO testA	testB	val	refCOCO+ testA	testB	refCOCOg val	test	Avg.
<i>Specialised Models</i>										
PolyFormer-L [CVPR23] [74]	BERT	90.4	92.9	87.2	85.0	89.8	78.0	85.8	85.9	86.9
UNINEXT-L [CVPR24] [56]	BERT	91.4	93.7	88.9	83.1	87.9	76.2	86.9	87.5	87.0
G-DINO [ECCV24] [55]	BERT	90.6	93.2	88.2	82.8	89.0	75.9	86.1	87.0	86.6
<i>Generalist Models (7B)</i>										
Shikra [Arxiv23] [58]	Vicuna-7B	87.0	90.6	80.2	81.6	87.4	72.1	82.3	82.2	82.9
Qwen2-VL [Arxiv24] [27]	Qwen2-7B	91.7	93.6	87.3	85.8	90.5	79.5	87.3	87.8	87.9
Qwen2.5-VL [Arxiv24] [44]	Qwen2.5-7B	90.0	92.5	85.4	84.2	89.1	76.9	87.2	87.2	86.6
InternVL2 [Arxiv24] [6]	InternLM2-7B	87.1	91.1	80.7	79.8	87.9	71.4	82.7	82.7	82.9
InternVL3 [Arxiv25] [29]	Qwen2.5-7B	<b>92.5</b>	<b>94.6</b>	88.0	<b>88.2</b>	<b>92.5</b>	<b>81.8</b>	<b>89.6</b>	<b>90.0</b>	<b>89.7</b>
LISA [CVPR24] [15]	Vicuna-7B	85.4	88.8	82.6	74.2	79.5	68.4	79.3	80.4	79.8
GSVA [CVPR24] [16]	Vicuna-7B	86.3	89.2	83.8	72.8	78.8	68.0	81.6	81.8	80.3
VistaLLM [CVPR24] [22]	Vicuna-7B	88.1	91.5	83.0	82.9	89.8	74.8	83.6	84.4	84.8
Groma [ECCV24] [10]	Vicuna-7B	89.5	92.1	86.3	83.9	88.9	78.1	86.4	87.0	86.5
SegLLM [ICLR25] [47]	Vicuna-7B	90.0	92.1	86.2	82.2	85.5	76.1	83.9	85.9	85.2
Text4Seg [25]	InternLM2-7B	90.3	93.4	87.5	85.2	89.9	79.5	85.4	85.4	87.1
Text4Seg++	Qwen2-7B	<b>93.2</b>	<b>95.3</b>	<b>90.7</b>	<b>89.7</b>	<b>93.2</b>	<b>84.5</b>	<b>90.8</b>	<b>91.2</b>	<b>91.1</b>
<i>Generalist Models (<math>\geq 13B</math>)</i>										
Shikra [Arxiv23] [58]	Vicuna-13B	87.8	91.1	81.8	82.9	87.8	74.4	82.6	83.2	84.0
LISA [CVPR24] [15]	LLaMA2-13B	85.9	88.8	81.7	74.5	80.6	68.3	80.1	81.3	80.2
GSVA [CVPR24] [16]	LLaMA2-13B	89.2	92.1	87.2	79.7	84.5	73.4	85.5	86.2	84.7
VistaLLM [CVPR24] [22]	Vicuna-13B	89.9	92.5	85.0	84.1	90.3	75.8	86.0	86.4	86.3
InternVL3 [Arxiv25] [29]	Qwen2.5-14B	<b>92.0</b>	<b>94.4</b>	87.8	<b>87.4</b>	<b>92.1</b>	<b>81.5</b>	<b>88.6</b>	<b>89.3</b>	<b>89.1</b>
Text4Seg [25]	Vicuna-13B	91.2	94.3	<b>88.0</b>	85.7	90.8	80.1	85.6	85.5	87.7
Text4Seg++	Qwen2.5-14B	<b>94.3</b>	<b>96.2</b>	<b>91.4</b>	<b>90.6</b>	<b>94.2</b>	<b>86.1</b>	<b>91.6</b>	<b>91.8</b>	<b>92.0</b>

TABLE X  
VISUAL QUESTION ANSWERING AND REFERRING EXPRESSION SEGMENTATION RESULTS ON VARIOUS BENCHMARKS. MIX<sup>†</sup> IS A COMBINATION OF REFERRING SEGMENTATION, SEMANTIC SEGMENTATION AND VQA DATASETS FROM LISA.

Method	LLM	Training Data	VQA						RES (val)		
			VQAv2	GQA	VisWiz	ScienceQA	TextQA	POPE	refCOCO	refCOCO+	refCOCOg
LISA [CVPR24] [15]	Vicuna-7B	Mix <sup>†</sup>	-	-	-	-	-	-	74.1	62.4	66.4
LLaVA-1.5 [CVPR24] [4]	Vicuna-7B	665k	78.0	61.7	50.6	68.4	55.0	85.4	-	-	-
Text4Seg [25]	Vicuna-7B	665k + refseg	76.6	60.2	50.9	68.1	55.0	84.2	77.5	70.7	73.4

Text4Seg++ consistently surpasses recent generalist MLLMs such as Qwen2-VL (87.9), VistaLLM (84.8), and SegLLM (85.2). Specifically, under 7B scale, Text4Seg++ obtains the best results on all evaluation splits, with an average of 91.1 that is significantly higher than existing SOTA method, *e.g.*, InternVL3 at 89.7. At the  $\geq 13B$  scale, Text4Seg++ further improves to an average score of 92.0, again outperforming prior best models such as InternVL3-14B (89.1) and GSVA (84.7). Notably, it achieves the best results on all splits, including 86.1 on RefCOCO+ testB, compared to 81.5 by InternVL3. These results highlight a key advantage of our unified formulation: by jointly modeling “where to look” and “what to segment”, Text4Seg++ benefits from dense mask supervision, which strengthens spatial understanding and significantly enhances grounding precision.

7) *Visual Understanding*: Our text-as-mask paradigm allows for seamless integration of downstream segmentation task into the pre-training of MLLMs. To evaluate its effectiveness, we assess the model’s performance on various visual understanding benchmarks, using the LLaVA-1.5-7B model as the baseline. Our method, Text4Seg, built upon the stage-2 of LLaVA-1.5-7B, is trained on both the LLaVA-v1.5-

mix665k dataset and our referring segmentation datasets. For a comprehensive comparison, we also report the performance of the LLaVA-1.5-7B model based on our implementation.

Table X presents a comprehensive comparison between LLaVA-1.5 and Text4Seg across various VQA and RES benchmarks. Notably, Text4Seg, trained on a mixed dataset, achieves performance on par with LLaVA-1.5 in visual question answering tasks while delivering strong results on RES benchmarks. These results validate that our text-as-mask based segmentation method acts as a seamless enhancement, offering a streamlined approach for pre-training MLLMs. It successfully integrates robust segmentation functionality without compromising the model’s conversational capabilities.

#### D. Visualization Analysis

We present qualitative comparisons between Text4Seg and GSVA in Figures 9 and 10 to highlight the effectiveness of our text-as-mask framework across different segmentation scenarios. In the single-object RES task, Text4Seg demonstrates a superior understanding of referring expressions, generating more accurate and precise segmentation maps compared to



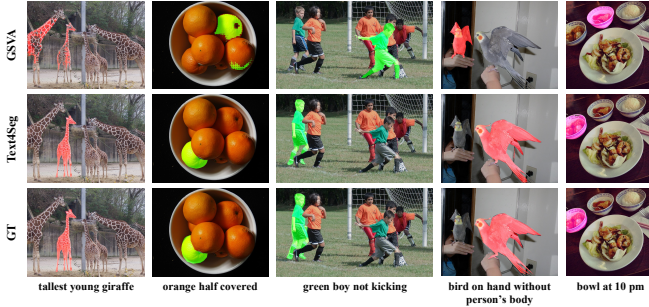


Fig. 9: Qualitative results of Text4Seg and GSVA [16] on the RES task. The corresponding referring expressions are displayed in the bottom.

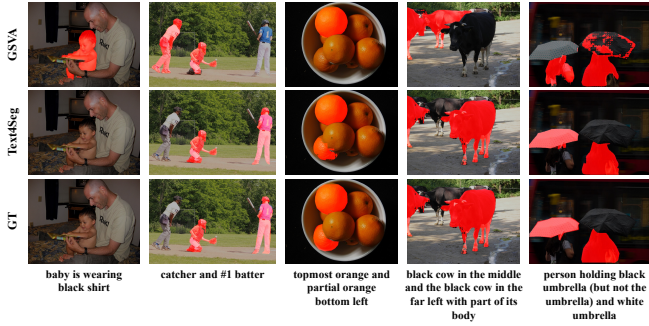


Fig. 10: Qualitative results of Text4Seg and GSVA [16] on the GRES task.

GSVA. In the GRES task (Figure 10), GSVA tends to incorrectly segment empty objects despite the inclusion of a `<REJ>` token (as seen in the first two columns). In contrast, Text4Seg consistently avoids such mistakes by labeling them as “others” without special design. Furthermore, Text4Seg significantly outperforms GSVA in the multiple-object RES task, delivering more precise segmentation results with better grounding performance. These results fully validate the effectiveness of Text4Seg in handling diverse and challenging visual grounding and segmentation tasks.

To further assess generalization and task versatility, we visualize qualitative results from Text4Seg++ across a wide range of vision-language segmentation tasks in Figure 11. These examples demonstrate that our enhanced model with box-wise semantic descriptors can effectively handle tasks that go beyond explicit referring expressions. For instance, in single-object reasoning segmentation from the ReasonSeg dataset and multi-object reasoning tasks from the MUSE benchmark, Text4Seg++ accurately segments semantically relevant regions using abstract region tags like “`roi0`, `roi1`, ...”, showcasing its capacity for implicit reasoning and compositional understanding. Moreover, in remote sensing tasks (last two rows), Text4Seg++ exhibits strong domain generalization, producing precise masks for complex aerial imagery. These results collectively highlight the versatility, robustness, and fine-grained segmentation capabilities of Text4Seg++ across both natural and geospatial domains, validating its unified and generative formulation for a broad spectrum of vision-language segmentation tasks.



Fig. 11: Qualitative results of Text4Seg++ across various vision-language tasks and diverse scenarios, including challenging tasks on remote sensing datasets.

## E. Ablation Study and Analysis

1) *Resolution of Semantic Descriptors*: To assess the impact of semantic descriptor granularity on segmentation performance, we construct instruction-tuning datasets using box-wise semantic descriptors at varying spatial resolutions, ranging from  $32 \times 32$  to  $80 \times 80$ . For reference, we also include the  $16 \times 16$  image-wise semantic descriptors configuration used in Text4Seg. As illustrated in Figure 12, higher-resolution semantic descriptors representations yield qualitatively finer segmentation outputs. Increasing the resolution leads to more precise object boundaries and improved structural detail. In contrast, lower-resolution settings, such as  $16 \times 16$ , exhibit blocky artifacts and under-segmentation due to coarse spatial encoding. Notably, the  $64^2$  or  $80^2$  configuration achieves segmentation quality that closely resembles results obtained with an external mask refiner like SAM.

These observations are quantitatively validated in Figure 13, where we report average cIoU scores across all splits of the RefCOCO, RefCOCO+, and RefCOCOg benchmarks. The results show a consistent improvement in performance as the resolution of the box-wise semantic descriptors increases. Importantly, the  $64 \times 64$  resolution already achieves parity, or even slightly outperforms, the SAM-refined variant of our model, indicating that dense and compact semantic tokens can drive high-quality segmentation in a fully generative manner. Given its strong balance between performance and sequence length, we adopt the  $64 \times 64$  resolution as the default setting in our experiments.

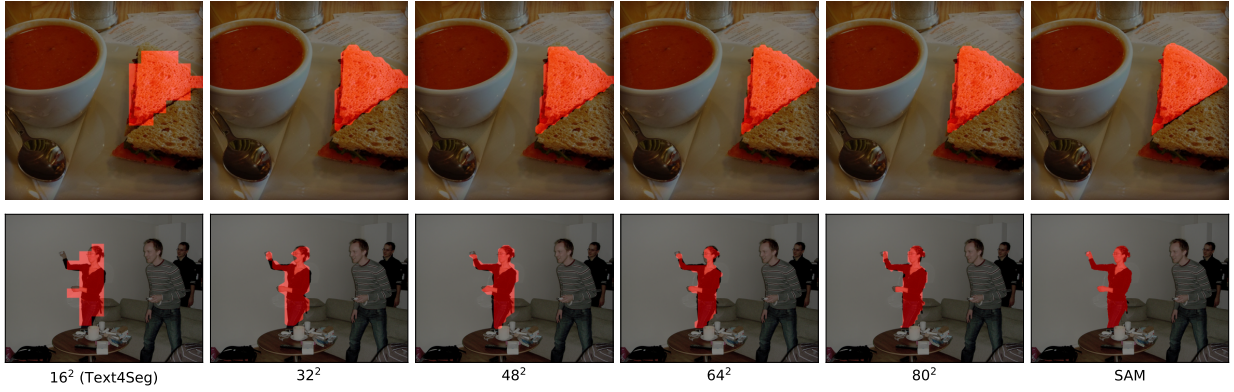


Fig. 12: Visualization of RES results across different resolutions, and with SAM as mask refiner.

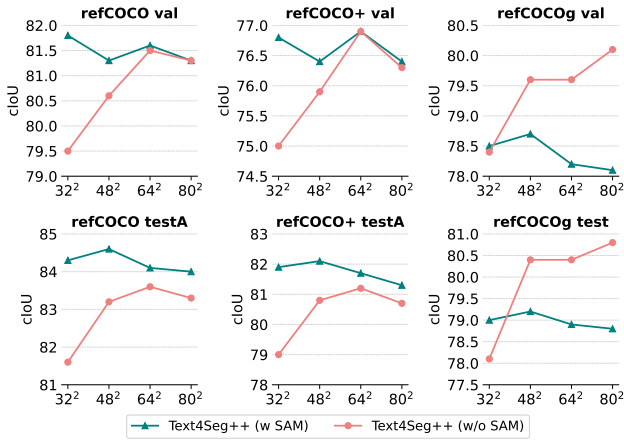


Fig. 13: Quantitative comparison of referring expression segmentation results using different resolutions of box-wise semantic descriptors.

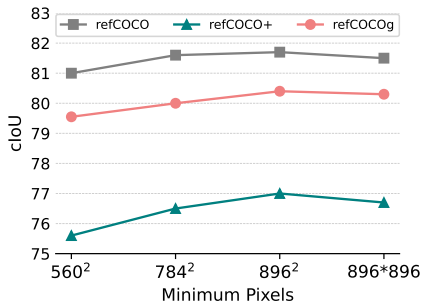


Fig. 14: Quantitative comparison of referring expression segmentation results with different image input resolutions. All images are resized to meet a specified minimum pixel count before being fed into the model.

2) *Resolution of Input Image*: Unlike most methods that leverage SAM’s image encoder, typically operating at high resolutions such as  $1024^2$ , paired with a mask decoder, Text4Seg++ performs segmentation solely through the vision-language modeling capabilities of MLLMs. As a result, its ability to perceive fine-grained visual details is directly influenced by the resolution of the input image, making it an important factor to investigate. To assess this impact, we evaluate Text4Seg++ across four different input resolutions. As shown in Figure 14, we report the average cIoU scores over the

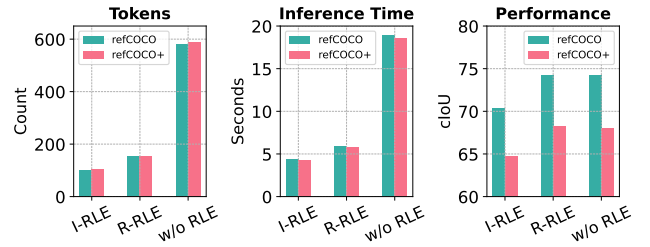


Fig. 15: Comparison of different encoding strategies for semantic descriptors at the  $16 \times 16$  resolution. Experiments are conducted on a standard NVIDIA V100 GPU. Our proposed Row-wise Run-Length Encoding (R-RLE) achieves an optimal trade-off between token efficiency, inference speed, and accuracy.

TABLE XI  
ABLATION RESULTS OF TEXT4SEG++ WITH AND WITHOUT SEMANTIC BRICKS (SB). RESULTS ARE REPORTED AS THE AVERAGE mIoU ACROSS ALL SPLITS OF EACH DATASET.

Method	SB	refCOCO	refCOCO+	refCOCOg
Text4Seg++	✗	79.7	74.9	78.1
Text4Seg++	✓	79.7	75.1	78.3

refCOCO, refCOCO+, and refCOCOg benchmarks. The results exhibit a clear trend: segmentation performance improves consistently as the input resolution increases, highlighting the critical role of high-resolution visual input in enhancing spatial understanding and mask quality. In particular, increasing resolution from  $560^2$  to  $896^2$  (while preserving the original aspect ratio) yields a notable accuracy boost. However, forcing the image into a square shape ( $896 \times 896$ ) introduces slight distortions and results in a marginal performance drop. Based on this trade-off between spatial fidelity and computational efficiency, we adopt  $784^2$  (minimum pixels with the native aspect ratio) as the default input resolution in all experiments.

3) *I-RLE v.s. R-RLE*: We investigate the impact of different encoding methods for semantic descriptors at a  $16 \times 16$  resolution using the train/val splits of the refCOCO and refCOCO+ datasets. As illustrated in Figure 15, while full-length semantic descriptors achieve high performance, they suffer from significantly longer inference times ( $\sim 19$  seconds) due to longer output tokens ( $\sim 590$ ) on both datasets. Although the I-RLE method reduces both the number of tokens and

inference time, it results in a notable performance drop, from 74.2 to 70.4 cIoU on refCOCO and 68.0 to 64.7 cIoU on refCOCO+. Our proposed R-RLE method strikes a better balance, reducing the length of semantic descriptors by 74% and improving inference speed by an average of  $3\times$ , while still maintaining nearly the same performance. These results highlight the effectiveness of R-RLE as an efficient yet lossless encoding mechanism for integrating dense segmentation into the generative pipeline of MLLMs.

4) *Ablation study about Semantic Bricks*: We assess the impact of Semantic Bricks (SB) by comparing Text4Seg++ with and without this component using the  $32\times 32$  box-wise semantic descriptors. As shown in Table XI, removing SB yields minimal changes in performance, but slightly degrades results on refCOCO+ and refCOCOg. This suggests that our box-wise semantic descriptor with semantic bricks provide minor yet consistent benefits. More importantly, as illustrated in Figure 7, Semantic Bricks significantly reduce the sequence length, enabling the use of higher-resolution B-SD ( $64\times 64$ ) for finer-grained segmentation while also accelerating both training and inference.

## V. DISCUSSION

### A. Conclusion

In this work, we presented text-as-mask, a novel paradigm that fundamentally recasts image segmentation as a text generation problem within Multimodal Large Language Models (MLLMs). This approach eliminates the need for additional decoders, simplifying the integration of dense prediction tasks. Our initial image-wise semantic descriptors provided a patch-aligned textual representation, enhanced by Row-wise Run-Length Encoding (RLE) for significant length reduction and inference speedup, forming the foundation of our Text4Seg framework. Building upon this, we further refined our approach with box-wise semantic descriptors. This more compact, region-level representation leverages bounding boxes and semantic bricks, leading to our next-brick prediction framework: Text4Seg++. Text4Seg++ not only achieves significantly finer-grained segmentation compared to its predecessor but also maintains a reduced sequence length, showcasing a powerful combination of precision, scalability, and generative efficiency. Extensive experiments across a wide range of benchmarks, including referring expression, reasoning, and challenging tasks like remote sensing segmentation, consistently demonstrated that Text4Seg++ surpasses existing state-of-the-art methods. Importantly, it achieves this superior performance without any task-specific fine-tuning or architectural modifications, showcasing its exceptional versatility and robustness across diverse domains and tasks.

### B. Future works and broader impact

Our work underscores the potential of treating dense prediction as a generative language modeling task. In the future, we believe that the *text-as-mask* paradigm opens promising new research directions for integrating fine-grained visual understanding into large-scale vision-language models in a principled, efficient, and generalizable manner.

## REFERENCES

- [1] S. Yin, C. Fu, S. Zhao, K. Li, X. Sun, T. Xu, and E. Chen, "A survey on multimodal large language models," *National Science Review*, vol. 11, no. 12, 2024.
- [2] H. Liu, C. Li, Q. Wu, and Y. J. Lee, "Visual instruction tuning," *Advances in neural information processing systems*, vol. 36, 2024.
- [3] H. Lu, W. Liu, B. Zhang, B. Wang, K. Dong, B. Liu, J. Sun, T. Ren, Z. Li, H. Yang, Y. Sun, C. Deng, H. Xu, Z. Xie, and C. Ruan, "Deepseek-vl: Towards real-world vision-language understanding," 2024.
- [4] H. Liu, C. Li, Y. Li, and Y. J. Lee, "Improved baselines with visual instruction tuning," in *Proceedings of the IEEE/CVF Conference on Computer Vision and Pattern Recognition*, 2024, pp. 26 296–26 306.
- [5] J. Bai, S. Bai, S. Yang, S. Wang, S. Tan, P. Wang, J. Lin, C. Zhou, and J. Zhou, "Qwen-vl: A versatile vision-language model for understanding, localization, text reading, and beyond," *arXiv preprint arXiv:2308.12966*, 2023.
- [6] Z. Chen, W. Wang, H. Tian, S. Ye, Z. Gao, E. Cui, W. Tong, K. Hu, J. Luo, S. Ma *et al.*, "How far are we to gpt-4v? closing the gap to commercial multimodal models with open-source suites," *Science China Information Sciences*, vol. 67, no. 12, p. 220101, 2024.
- [7] K. Song, Y. Zhu, B. Liu, Q. Yan, A. Elgammal, and X. Yang, "Moma: Multimodal llm adapter for fast personalized image generation," in *European Conference on Computer Vision*. Springer, 2024, pp. 117–132.
- [8] Z. Wang, A. Li, Z. Li, and X. Liu, "Genartist: Multimodal llm as an agent for unified image generation and editing," *Advances in Neural Information Processing Systems*, vol. 37, pp. 128 374–128 395, 2024.
- [9] W. Wang, Z. Chen, X. Chen, J. Wu, X. Zhu, G. Zeng, P. Luo, T. Lu, J. Zhou, Y. Qiao *et al.*, "Visionllm: Large language model is also an open-ended decoder for vision-centric tasks," *Advances in Neural Information Processing Systems*, vol. 36, 2024.
- [10] C. Ma, Y. Jiang, J. Wu, Z. Yuan, and X. Qi, "Groma: Localized visual tokenization for grounding multimodal large language models," in *European Conference on Computer Vision*. Springer, 2024, pp. 417–435.
- [11] J. Wu, X. Li, S. Xu, H. Yuan, H. Ding, Y. Yang, X. Li, J. Zhang, Y. Tong, X. Jiang *et al.*, "Towards open vocabulary learning: A survey," *IEEE Transactions on Pattern Analysis and Machine Intelligence*, vol. 46, no. 7, pp. 5092–5113, 2024.
- [12] A. Zhang, L. Zhao, C.-W. Xie, Y. Zheng, W. Ji, and T.-S. Chua, "Nextchat: An lmm for chat, detection and segmentation," *arXiv preprint arXiv:2311.04498*, 2023.
- [13] X. Li, H. Ding, H. Yuan, W. Zhang, J. Pang, G. Cheng, K. Chen, Z. Liu, and C. C. Loy, "Transformer-based visual segmentation: A survey," *IEEE transactions on pattern analysis and machine intelligence*, 2024.
- [14] M. Lan, X. Wang, Y. Ke, J. Xu, L. Feng, and W. Zhang, "Smoosseg: smoothness prior for unsupervised semantic segmentation," *Advances in Neural Information Processing Systems*, vol. 36, pp. 11 353–11 373, 2023.
- [15] X. Lai, Z. Tian, Y. Chen, Y. Li, Y. Yuan, S. Liu, and J. Jia, "Lisa: Reasoning segmentation via large language model," in *Proceedings of the IEEE/CVF Conference on Computer Vision and Pattern Recognition*, 2024, pp. 9579–9589.
- [16] Z. Xia, D. Han, Y. Han, X. Pan, S. Song, and G. Huang, "Gsva: Generalized segmentation via multimodal large language models," in *Proceedings of the IEEE/CVF Conference on Computer Vision and Pattern Recognition*, 2024, pp. 3858–3869.
- [17] Y. Zhang, Z. Ma, X. Gao, S. Shakhia, Q. Gao, and J. Chai, "Groundhog: Grounding large language models to holistic segmentation," in *Proceedings of the IEEE/CVF conference on computer vision and pattern recognition*, 2024, pp. 14 227–14 238.
- [18] J. He, Y. Wang, L. Wang, H. Lu, J.-Y. He, J.-P. Lan, B. Luo, and X. Xie, "Multi-modal instruction tuned llms with fine-grained visual perception," in *Proceedings of the IEEE/CVF Conference on Computer Vision and Pattern Recognition*, 2024, pp. 13 980–13 990.
- [19] Z. Ren, Z. Huang, Y. Wei, Y. Zhao, D. Fu, J. Feng, and X. Jin, "Pixellm: Pixel reasoning with large multimodal model," in *Proceedings of the IEEE/CVF Conference on Computer Vision and Pattern Recognition*, 2024, pp. 26 374–26 383.
- [20] H. Rasheed, M. Maaz, S. Shaji, A. Shaker, S. Khan, H. Cholakkal, R. M. Anwer, E. Xing, M.-H. Yang, and F. S. Khan, "Glamm: Pixel grounding large multimodal model," in *Proceedings of the IEEE/CVF Conference on Computer Vision and Pattern Recognition*, 2024, pp. 13 009–13 018.
- [21] A. Kirillov, E. Mintun, N. Ravi, H. Mao, C. Rolland, L. Gustafson, T. Xiao, S. Whitehead, A. C. Berg, W.-Y. Lo *et al.*, "Segment anything,"



- in *Proceedings of the IEEE/CVF International Conference on Computer Vision*, 2023, pp. 4015–4026.
- [22] S. Pramanick, G. Han, R. Hou, S. Nag, S.-N. Lim, N. Ballas, Q. Wang, R. Chellappa, and A. Almahairi, “Jack of all tasks master of many: Designing general-purpose coarse-to-fine vision-language model,” in *Proceedings of the IEEE/CVF Conference on Computer Vision and Pattern Recognition*, 2024, pp. 14 076–14 088.
  - [23] B. Xiao, H. Wu, W. Xu, X. Dai, H. Hu, Y. Lu, M. Zeng, C. Liu, and L. Yuan, “Florence-2: Advancing a unified representation for a variety of vision tasks,” in *Proceedings of the IEEE/CVF Conference on Computer Vision and Pattern Recognition*, 2024, pp. 4818–4829.
  - [24] J. Wu, M. Zhong, S. Xing, Z. Lai, Z. Liu, Z. Chen, W. Wang, X. Zhu, L. Lu, T. Lu *et al.*, “Visionllm v2: An end-to-end generalist multimodal large language model for hundreds of vision-language tasks,” *Advances in Neural Information Processing Systems*, vol. 37, pp. 69 925–69 975, 2024.
  - [25] M. Lan, C. Chen, Y. Zhou, J. Xu, Y. Ke, X. Wang, L. Feng, and W. Zhang, “Text4seg: Reimagining image segmentation as text generation,” in *The Thirteenth International Conference on Learning Representations*, 2025. [Online]. Available: <https://openreview.net/forum?id=vkakKdzNF5>
  - [26] A. Dosovitskiy, L. Beyer, A. Kolesnikov, D. Weissenborn, X. Zhai, T. Unterthiner, M. Dehghani, M. Minderer, G. Heigold, S. Gelly, J. Uszkoreit, and N. Houlsby, “An image is worth 16x16 words: Transformers for image recognition at scale,” in *International Conference on Learning Representations*, 2021. [Online]. Available: <https://openreview.net/forum?id=YicbFdNTTy>
  - [27] P. Wang, S. Bai, S. Tan, S. Wang, S. Fan, J. Bai, K. Chen, X. Liu, J. Wang, W. Ge *et al.*, “Qwen2-vl: Enhancing vision-language model’s perception of the world at any resolution,” *arXiv preprint arXiv:2409.12191*, 2024.
  - [28] Z. Wu, X. Chen, Z. Pan, X. Liu, W. Liu, D. Dai, H. Gao, Y. Ma, C. Wu, B. Wang *et al.*, “Deepseek-vl2: Mixture-of-experts vision-language models for advanced multimodal understanding,” *arXiv preprint arXiv:2412.10302*, 2024.
  - [29] J. Zhu, W. Wang, Z. Chen, Z. Liu, S. Ye, L. Gu, Y. Duan, H. Tian, W. Su, J. Shao *et al.*, “Internvl3: Exploring advanced training and test-time recipes for open-source multimodal models,” *arXiv preprint arXiv:2504.10479*, 2025.
  - [30] J.-B. Alayrac, J. Donahue, P. Luc, A. Miech, I. Barr, Y. Hasson, K. Lenc, A. Mensch, K. Millican, M. Reynolds *et al.*, “Flamingo: a visual language model for few-shot learning,” *Advances in neural information processing systems*, vol. 35, pp. 23 716–23 736, 2022.
  - [31] A. Awadalla, I. Gao, J. Gardner, J. Hessel, Y. Hanafy, W. Zhu, K. Marathe, Y. Bitton, S. Gadre, S. Sagawa *et al.*, “Openflamingo: An open-source framework for training large autoregressive vision-language models,” *arXiv preprint arXiv:2308.01390*, 2023.
  - [32] B. Li, Y. Zhang, L. Chen, J. Wang, F. Pu, J. A. Cahyono, J. Yang, C. Li, and Z. Liu, “Otter: A multi-modal model with in-context instruction tuning,” *IEEE Transactions on Pattern Analysis and Machine Intelligence*, 2025.
  - [33] J. Li, D. Li, S. Savarese, and S. Hoi, “Blip-2: Bootstrapping language-image pre-training with frozen image encoders and large language models,” in *International conference on machine learning*. PMLR, 2023, pp. 19 730–19 742.
  - [34] W. Dai, J. Li, D. Li, A. Tiong, J. Zhao, W. Wang, B. Li, P. Fung, and S. Hoi, “InstructBLIP: Towards general-purpose vision-language models with instruction tuning,” in *Thirty-seventh Conference on Neural Information Processing Systems*, 2023. [Online]. Available: <https://openreview.net/forum?id=vvoWPYqZJA>
  - [35] Q. Ye, H. Xu, J. Ye, M. Yan, A. Hu, H. Liu, Q. Qian, J. Zhang, and F. Huang, “mplug-owl2: Revolutionizing multi-modal large language model with modality collaboration,” in *Proceedings of the IEEE/CVF Conference on Computer Vision and Pattern Recognition*, 2024, pp. 13 040–13 051.
  - [36] H. Liu, C. Li, Y. Li, B. Li, Y. Zhang, S. Shen, and Y. J. Lee, “Llava-next: Improved reasoning, ocr, and world knowledge,” 2024.
  - [37] Z. Guo, R. Xu, Y. Yao, J. Cui, Z. Ni, C. Ge, T.-S. Chua, Z. Liu, and G. Huang, “Llava-uhd: an Imm perceiving any aspect ratio and high-resolution images,” in *European Conference on Computer Vision*. Springer, 2024, pp. 390–406.
  - [38] B. Li, Y. Zhang, D. Guo, R. Zhang, F. Li, H. Zhang, K. Zhang, P. Zhang, Y. Li, Z. Liu, and C. Li, “LLaVA-onevision: Easy visual task transfer,” *Transactions on Machine Learning Research*, 2025. [Online]. Available: <https://openreview.net/forum?id=zKv8qULV6n>
  - [39] Y. Li, Y. Zhang, C. Wang, Z. Zhong, Y. Chen, R. Chu, S. Liu, and J. Jia, “Mini-gemini: Mining the potential of multi-modality vision language models,” *arXiv preprint arXiv:2403.18814*, 2024.
  - [40] Z. Li, B. Yang, Q. Liu, Z. Ma, S. Zhang, J. Yang, Y. Sun, Y. Liu, and X. Bai, “Monkey: Image resolution and text label are important things for large multi-modal models,” in *Proceedings of the IEEE/CVF Conference on Computer Vision and Pattern Recognition*, 2024, pp. 26 763–26 773.
  - [41] Z. Lin, D. Liu, R. Zhang, P. Gao, L. Qiu, H. Xiao, H. Qiu, W. Shao, K. Chen, J. Han *et al.*, “Sphinx: A mixer of weights, visual embeddings and image scales for multi-modal large language models,” in *European Conference on Computer Vision*. Springer, 2024, pp. 36–55.
  - [42] C. Wei, Y. Zhong, H. Tan, Y. Zeng, Y. Liu, Z. Zhao, and Y. Yang, “Instructseg: Unifying instructed visual segmentation with multi-modal large language models,” *arXiv preprint arXiv:2412.14006*, 2024.
  - [43] Z. Chen, W. Wang, Y. Cao, Y. Liu, Z. Gao, E. Cui, J. Zhu, S. Ye, H. Tian, Z. Liu *et al.*, “Expanding performance boundaries of open-source multimodal models with model, data, and test-time scaling,” *arXiv preprint arXiv:2412.05271*, 2024.
  - [44] S. Bai, K. Chen, X. Liu, J. Wang, W. Ge, S. Song, K. Dang, P. Wang, S. Wang, J. Tang *et al.*, “Qwen2.5-vl technical report,” *arXiv preprint arXiv:2502.13923*, 2025.
  - [45] T. Zhang, X. Li, H. Fei, H. Yuan, S. Wu, S. Ji, C. C. Loy, and S. Yan, “Omg-llava: Bridging image-level, object-level, pixel-level reasoning and understanding,” *Advances in Neural Information Processing Systems*, vol. 37, pp. 71 737–71 767, 2024.
  - [46] D. Jang, Y. Cho, S. Lee, T. Kim, and D. Kim, “MMR: A large-scale benchmark dataset for multi-target and multi-granularity reasoning segmentation,” in *The Thirteenth International Conference on Learning Representations*, 2025. [Online]. Available: <https://openreview.net/forum?id=mzL19kKE3r>
  - [47] X. Wang, S. Zhang, S. Li, K. Li, K. Kallidromitis, Y. Kato, K. Kozuka, and T. Darrell, “SegLLM: Multi-round reasoning segmentation with large language models,” in *The Thirteenth International Conference on Learning Representations*, 2025. [Online]. Available: <https://openreview.net/forum?id=Pm1NXHgzYf>
  - [48] K. Li, Z. Xin, L. Pang, C. Pang, Y. Deng, J. Yao, G. Xia, D. Meng, Z. Wang, and X. Cao, “Segearth-r1: Geospatial pixel reasoning via large language model,” *arXiv preprint arXiv:2504.09644*, 2025.
  - [49] R. Ou, Y. Hu, F. Zhang, J. Chen, and Y. Liu, “Geopix: A multimodal large language model for pixel-level image understanding in remote sensing,” *IEEE Geoscience and Remote Sensing Magazine*, 2025.
  - [50] H. Tang, C. Xie, H. Wang, X. Bao, T. Weng, P. Li, Y. Zheng, and L. Wang, “Ufo: A unified approach to fine-grained visual perception via open-ended language interface,” *arXiv preprint arXiv:2503.01342*, 2025.
  - [51] T. Zhang, X. Li, Z. Huang, Y. Li, W. Lei, X. Deng, S. Chen, S. Ji, and J. Feng, “Pixel-sail: Single transformer for pixel-grounded understanding,” *arXiv preprint arXiv:2504.10465*, 2025.
  - [52] T. Wang, C. Cheng, L. Wang, S. Chen, and W. Zhao, “Himtok: Learning hierarchical mask tokens for image segmentation with large multimodal model,” *arXiv preprint arXiv:2503.13026*, 2025.
  - [53] L. Wang, H. Lin, S. Chen, T. Wang, C. Cheng, Y. Zhong, D. Zheng, and W. Zhao, “Alto: Adaptive-length tokenizer for autoregressive mask generation,” *arXiv preprint arXiv:2505.16495*, 2025.
  - [54] T. Chen, S. Saxena, L. Li, D. J. Fleet, and G. Hinton, “Pix2seq: A language modeling framework for object detection,” in *International Conference on Learning Representations*, 2022. [Online]. Available: <https://openreview.net/forum?id=e42Kblw6Wb>
  - [55] S. Liu, Z. Zeng, T. Ren, F. Li, H. Zhang, J. Yang, Q. Jiang, C. Li, J. Yang, H. Su *et al.*, “Grounding dino: Marrying dino with grounded pre-training for open-set object detection,” in *European Conference on Computer Vision*. Springer, 2024, pp. 38–55.
  - [56] B. Yan, Y. Jiang, J. Wu, D. Wang, P. Luo, Z. Yuan, and H. Lu, “Universal instance perception as object discovery and retrieval,” in *Proceedings of the IEEE/CVF Conference on Computer Vision and Pattern Recognition*, 2023, pp. 15 325–15 336.
  - [57] Z. Peng, W. Wang, L. Dong, Y. Hao, S. Huang, S. Ma, Q. Ye, and F. Wei, “Grounding multimodal large language models to the world,” in *The Twelfth International Conference on Learning Representations*, 2024. [Online]. Available: <https://openreview.net/forum?id=ILmqkxfSIw>
  - [58] K. Chen, Z. Zhang, W. Zeng, R. Zhang, F. Zhu, and R. Zhao, “Shikra: Unleashing multimodal llm’s referential dialogue magic,” *arXiv preprint arXiv:2306.15195*, 2023.
  - [59] H. Fei, S. Wu, H. Zhang, T.-S. Chua, and S. Yan, “Vitron: A unified pixel-level vision llm for understanding, generating, segmenting, editing,” 2024.

- [60] A. Radford, J. W. Kim, C. Hallacy, A. Ramesh, G. Goh, S. Agarwal, G. Sastry, A. Askell, P. Mishkin, J. Clark *et al.*, "Learning transferable visual models from natural language supervision," in *International conference on machine learning*. PmLR, 2021, pp. 8748–8763.
- [61] X. Zhai, B. Mustafa, A. Kolesnikov, and L. Beyer, "Sigmoid loss for language image pre-training," in *Proceedings of the IEEE/CVF international conference on computer vision*, 2023, pp. 11 975–11 986.
- [62] A. Yang, A. Li, B. Yang, B. Zhang, B. Hui, B. Zheng, B. Yu, C. Gao, C. Huang, C. Lv *et al.*, "Qwen3 technical report," *arXiv preprint arXiv:2505.09388*, 2025.
- [63] H. Touvron, T. Lavril, G. Izacard, X. Martinet, M.-A. Lachaux, T. Lacroix, B. Rozière, N. Goyal, E. Hambro, F. Azhar *et al.*, "Llama: Open and efficient foundation language models," *arXiv preprint arXiv:2302.13971*, 2023.
- [64] S. Kazemzadeh, V. Ordonez, M. Matten, and T. Berg, "Referitgame: Referring to objects in photographs of natural scenes," in *Proceedings of the 2014 conference on empirical methods in natural language processing (EMNLP)*, 2014, pp. 787–798.
- [65] S. Golomb, "Run-length encodings (corresp.)," *IEEE transactions on information theory*, vol. 12, no. 3, pp. 399–401, 1966.
- [66] E. J. Hu, Yelong shen, P. Wallis, Z. Allen-Zhu, Y. Li, S. Wang, L. Wang, and W. Chen, "LoRA: Low-rank adaptation of large language models," in *International Conference on Learning Representations*, 2022. [Online]. Available: <https://openreview.net/forum?id=nZeVKeeFYf9>
- [67] Y. Lin, H. Li, W. Shao, Z. Yang, J. Zhao, X. He, P. Luo, and K. Zhang, "SAMRefiner: Taming segment anything model for universal mask refinement," in *The Thirteenth International Conference on Learning Representations*, 2025. [Online]. Available: <https://openreview.net/forum?id=JIDx2xp01W>
- [68] Y. Zhao, J. Huang, J. Hu, X. Wang, Y. Mao, D. Zhang, Z. Jiang, Z. Wu, B. Ai, A. Wang, W. Zhou, and Y. Chen, "Swift: A scalable lightweight infrastructure for fine-tuning," in *AAAI*, 2025, pp. 29 733–29 735. [Online]. Available: <https://doi.org/10.1609/aaai.v39i28.35383>
- [69] I. Loshchilov and F. Hutter, "Decoupled weight decay regularization," in *International Conference on Learning Representations*, 2019. [Online]. Available: <https://openreview.net/forum?id=Bkg6RiCqY7>
- [70] S. Rajbhandari, J. Rasley, O. Ruwase, and Y. He, "Zero: Memory optimizations toward training trillion parameter models," in *SC20: International Conference for High Performance Computing, Networking, Storage and Analysis*. IEEE, 2020, pp. 1–16.
- [71] C. Wu, Z. Lin, S. Cohen, T. Bui, and S. Maji, "Phrasecut: Language-based image segmentation in the wild," in *Proceedings of the IEEE/CVF Conference on Computer Vision and Pattern Recognition*, 2020, pp. 10 216–10 225.
- [72] C. Liu, H. Ding, and X. Jiang, "Gres: Generalized referring expression segmentation," in *Proceedings of the IEEE/CVF conference on computer vision and pattern recognition*, 2023, pp. 23 592–23 601.
- [73] J. Mao, J. Huang, A. Toshev, O. Camburu, A. L. Yuille, and K. Murphy, "Generation and comprehension of unambiguous object descriptions," in *Proceedings of the IEEE conference on computer vision and pattern recognition*, 2016, pp. 11–20.
- [74] J. Liu, H. Ding, Z. Cai, Y. Zhang, R. K. Satzoda, V. Mahadevan, and R. Manmatha, "Polyformer: Referring image segmentation as sequential polygon generation," in *Proceedings of the IEEE/CVF Conference on Computer Vision and Pattern Recognition*, 2023, pp. 18 653–18 663.
- [75] Z. Yang, J. Wang, X. Ye, Y. Tang, K. Chen, H. Zhao, and P. H. Torr, "Language-aware vision transformer for referring segmentation," *IEEE Transactions on Pattern Analysis and Machine Intelligence*, 2024.
- [76] Y.-C. Chen, W.-H. Li, C. Sun, Y.-C. F. Wang, and C.-S. Chen, "Sam4mllm: Enhance multi-modal large language model for referring expression segmentation," in *European Conference on Computer Vision*. Springer, 2024, pp. 323–340.
- [77] M. Zhu, Y. Tian, H. Chen, C. Zhou, Q. Guo, Y. Liu, M. Yang, and C. Shen, "Segagent: Exploring pixel understanding capabilities in mllms by imitating human annotator trajectories," in *Proceedings of the Computer Vision and Pattern Recognition Conference*, 2025, pp. 3686–3696.
- [78] L. Zhu, T. Chen, Q. Xu, X. Liu, D. Ji, H. Wu, D. W. Soh, and J. Liu, "Popen: Preference-based optimization and ensemble for lvlm-based reasoning segmentation," in *Proceedings of the Computer Vision and Pattern Recognition Conference*, 2025, pp. 30 231–30 240.
- [79] T.-Y. Lin, M. Maire, S. Belongie, J. Hays, P. Perona, D. Ramanan, P. Dollár, and C. L. Zitnick, "Microsoft coco: Common objects in context," in *Computer vision—ECCV 2014: 13th European conference, zurich, Switzerland, September 6–12, 2014, proceedings, part v 13*. Springer, 2014, pp. 740–755.
- [80] Z. You, J. Wang, L. Kong, B. He, and Z. Wu, "Pix2cap-coco: Advancing visual comprehension via pixel-level captioning," *arXiv preprint arXiv:2501.13893*, 2025.
- [81] S. Liu, Y. Ma, X. Zhang, H. Wang, J. Ji, X. Sun, and R. Ji, "Rotated multi-scale interaction network for referring remote sensing image segmentation," in *Proceedings of the IEEE/CVF Conference on Computer Vision and Pattern Recognition*, 2024, pp. 26 658–26 668.
- [82] Y. Liu, B. Peng, Z. Zhong, Z. Yue, F. Lu, B. Yu, and J. Jia, "Seg-zero: Reasoning-chain guided segmentation via cognitive reinforcement," *arXiv preprint arXiv:2503.06520*, 2025.
- [83] M. Lan, C. Chen, Y. Ke, X. Wang, L. Feng, and W. Zhang, "Clearclip: Decomposing clip representations for dense vision-language inference," in *European Conference on Computer Vision*. Springer, 2024, pp. 143–160.
- [84] —, "Proxyclick: Proxy attention improves clip for open-vocabulary segmentation," in *European Conference on Computer Vision*. Springer, 2024, pp. 70–88.
- [85] Z. Ding, J. Wang, and Z. Tu, "Open-vocabulary universal image segmentation with maskclip," in *Proceedings of the 40th International Conference on Machine Learning*, ser. ICML'23. JMLR.org, 2023.
- [86] J. Xu, S. De Mello, S. Liu, W. Byeon, T. Breuel, J. Kautz, and X. Wang, "Groupvit: Semantic segmentation emerges from text supervision," in *Proceedings of the IEEE/CVF Conference on Computer Vision and Pattern Recognition*, 2022, pp. 18 134–18 144.
- [87] F. Liang, B. Wu, X. Dai, K. Li, Y. Zhao, H. Zhang, P. Zhang, P. Vajda, and D. Marculescu, "Open-vocabulary semantic segmentation with mask-adapted clip," in *Proceedings of the IEEE/CVF Conference on Computer Vision and Pattern Recognition*, 2023, pp. 7061–7070.
- [88] M. Xu, Z. Zhang, F. Wei, H. Hu, and X. Bai, "San: side adapter network for open-vocabulary semantic segmentation," *IEEE Transactions on Pattern Analysis and Machine Intelligence*, vol. 45, no. 12, pp. 15 546–15 561, 2023.
- [89] C. Wei, H. Tan, Y. Zhong, Y. Yang, and L. Ma, "Lasagna: Language-based segmentation assistant for complex queries," *arXiv preprint arXiv:2404.08506*, 2024.
- [90] Y. Zhou, M. Lan, X. Li, Y. Ke, X. Jiang, L. Feng, and W. Zhang, "Geoground: A unified large vision-language model. for remote sensing visual grounding," *arXiv preprint arXiv:2411.11904*, 2024.
- [91] B. Zhou, H. Zhao, X. Puig, T. Xiao, S. Fidler, A. Barriuso, and A. Torralba, "Semantic understanding of scenes through the ade20k dataset," *International Journal of Computer Vision*, vol. 127, pp. 302–321, 2019.
- [92] R. Mottaghi, X. Chen, X. Liu, N.-G. Cho, S.-W. Lee, S. Fidler, R. Urtasun, and A. Yuille, "The role of context for object detection and semantic segmentation in the wild," in *Proceedings of the IEEE conference on computer vision and pattern recognition*, 2014, pp. 891–898.
- [93] M. Everingham, "The pascal visual object classes challenge 2007," in <http://www.pascal-network.org/challenges/VOC/voc2007/workshop/index.html>, 2009.
- [94] M. Xu, Z. Zhang, F. Wei, H. Hu, and X. Bai, "Side adapter network for open-vocabulary semantic segmentation," in *Proceedings of the IEEE/CVF Conference on Computer Vision and Pattern Recognition*, 2023, pp. 2945–2954.